First Joint Chinese-Danish Symposium: Characterisation of Microstructures. Extended abstracts

Bowen, Jacob R.; Godfrey, A.; Pantleon, Wolfgang

Publication date:
2002

Document Version
Publisher's PDF, also known as Version of record

Risø-R-1347(EN)

First Joint Chinese-Danish Symposium: Characterisation of Microstructures Extended Abstracts

Editors:

Jacob R. Bowen
Andy Godfrey
Wolfgang Pantleon

Risø National Laboratory, Roskilde
August 2002

Abstract *The First Chinese-Danish Symposium on the Characterisation of Microstructures was held in Qinhuangdao, Hebei, China between 19-20 August 2002. This symposium was organised together with the closely related Summer School on the Geometry of Microstructures, which was held immediately prior to this symposium. At the symposium 29 lectures were presented and this document collects the extended abstracts from these presentations. The symposium was organised in six sessions: two on the characterisation of deformation microstructures, one on the characterisation of recrystallisation and three sessions describing the state-of-the-art of the available metallurgical techniques for the characterisation of the microstructures that occur as a result of thermomechanical processes. Under the theme of deformation, papers were presented on microstructure resulting from conventional forming processes as well as nano scale microstructures in metals such as aluminium and steel alloys produced by techniques such as surface mechanical attrition and equal channel angular extrusion. Classical aspects of recrystallisation such as stereology were presented which were then extrapolated for use in automated characterisation techniques, namely EBSP and 3DXRD, and in the same context the novel effects of magnetic and electric fields on recrystallisation phenomena were also discussed. Three main techniques were intensely investigated, namely TEM, EBSD and 3DXRD and occupied half of the scope and time of the symposium. Papers ranged from cautionary notes on the use of established techniques (TEM and EBSP) to exploratory studies on the capability of the novel 3DXRD technique. This symposium provided a platform for the open discussion between Chinese and Danish scientists on various metallic microstructures and related phenomena riding on the back of a school acutely focused on the theories behind the available characterisation tools. Therefore, this report provides a snapshot of Chinese and Danish scientific efforts in the field.*

ISBN 87-550-3072-6; ISBN 87-550-3073-4(Internet)
ISSN 0106-2840

Print: Pitney Bowes Management Services Danmark A/S, 2002

Contents

Preface

During the period 16 – 20 August, 2002, a Summer School on Geometry of Microstructures and the First Joint Danish-Chinese Materials Science Symposium on Characterisation of Microstructures were held in Qinhuangdao in China. This double event was organised by the Center for Fundamental Research: Metal Structures in Four Dimensions, Risø National Laboratory, Denmark, in collaboration with Tsinghua University and Yanshan University, China.

The themes of the School and Symposium were selected to supplement each other. The idea was that the School should provide the necessary background on theory, analysis methods as well as techniques and the Symposium should document how these tools are used at International level research. It turned out that this combination worked perfectly and was fruitful to all participants.

For the School, experienced lecturers were chosen to teach on the selected topics:

Boundaries	*Prof. Brian Ralph*
Stochastic Geometry / Stereology	*Prof. Krysztof Kurzydłowski*
Orientations	*Prof. Adam Morawiec*
Textures	*Prof. Weimin Mao*
Microstructures in TEM	*Dr. Claire Barlow*
High Spatial Resolution and Analytical EM	*Prof. Jing Zhu*

Lecture notes covering 178 pages were distributed to the participants. We were in total 65 participants: 17 Danish students from the Center, DTU, KU, AU and AAU, 8 Danish scientists, 22 Chinese students from 8 universities, 1 Polish student and 11 Chinese scientists as well as the 6 lecturers from China, Poland and the United Kingdom mentioned above. All students and essentially all scientists and lecturers stayed during the whole week and participated in both the School and Symposium. This created a very lively atmosphere with many discussions between Danish and Chinese scientists and students, etc. thus forming a basis for future scientific projects and collaborations as well as new friendships.

This report contains the programme and the extended abstracts from the presentations during the Symposium. These abstracts cover advanced experimental techniques for microstructural characterisation as well as data analysis and interpretation methods for determining the important parameters, which quantifies the relevant elements of the microstructure. Focus is on experimental aspects and modelling of plastic deformation and recrystallisation. Within these topics, Danish and Chinese scientists presented work, which is state-of-the-art internationally and it was demonstrated that fruitful collaboration is a realistic goal for the future.

I wish to thank all those at Tsinghua, Yanshan and Risø, who have assisted in the preparations of the School and Symposium and bringing it to a successful completion. The financial support from the Chinese National Science Foundation and the Danish National Research Foundation is also gratefully acknowledged.

Dorte Juul Jensen
Head of Center for Fundamental Research:
Metal Structures in Four Dimensions

Five of the six lecturers of the Summer School. From the left: Weimin Mao, Claire Barlow, Adam Morawiec, Brian Ralph and Krysztof Kurzydłowski.

All of the students and postdoc's that were at the Summer School and Symposium.

First Joint Danish-Chinese Symposium

CHARACTERIZATION OF MICROSTRUCTURES

19-20 August 2002
in
Qinghuangdao
People's Republic of China

Organized by
Center for Fundamental Research:

Metal Structures
in
4D

in collaboration with
Tsinghua University and Janshan University

Advisory Committee:

Niels Hansen
Dorte Juul Jensen
Ke Lu
Brian Ralph
Zuqing Sun
Roy Vandermeer
Jing Zhu
Liang Zuo

Organization Committee:

Jacob R. Bowen
Andy Godfrey
Xiaoxu Huang
Dorte Juul Jensen
Qing Liu
Weimin Mao
Lesley Marcher
Wolfgang Pantleon
Xiang Zhao

This document can be downloaded from the Internet in PDF format.
http://www.risoe.dk/rispubl/AFM/Ris-R-1347.pdf
More information about the Center can be found on the Internet.
http://www.metals4d.dk/

List of Participants

Claire Barlow
Institute of Manufacturing
Cambridge University
Engineering Department
Mill Lane
Cambridge
CB2-1RX
United Kingdom
cyb@eng.cam.ac.uk

Jacob R. Bowen
Center for Fundamental Research:
Metal Structures in Four
Dimensions
Materials Research Department
Risø National Laboratory
P.O. Box 49
4000 Roskilde
Denmark
jacob.r.bowen@risoe.dk

Wei Cai
School of Materials Science and
Engineering
Harbin Institute of Technology
Harbin 150001
P.R. China
weicai@hope.hit.edu.cn

Wenquan Cao
Department Materials Science and
Engineering
Tsinghua University
Beijing 100084
P.R. China
caowenquan00@mails.tsinghua.edu.cn

Jesper Christiansen
CAMP, Department of Physics
Building 307
Technical University of Denmark
DK-2800 Lyngby
Denmark
jeschris@fysik.dtu.dk

Kristian Vinter Dahl
IPL, Building 204
Technical University of Denmark
DK-2800 Lyngby
Denmark
c961016@student.dtu.dk

Elzbieta Fortuna
Department of Materials Science
and Engineering
Warsaw University of Technology
Wołoska 141
02-507 Warsaw
Poland
elaf@immat.pw.edu.pl

Morten Foversho
H. C. Ørsted Institute
University of Copenhagen
Denmark
mfo@fys.ku.dk

Xiaowei Fu
Center for Fundamental Research:
Metal Structures in Four
Dimensions
Materials Research Department
Risø National Laboratory
P.O. Box 49
4000 Roskilde
Denmark
xiaowei.fu@risoe.dk

Alex David Givskov
Department of Chemistry
University of Copenhagen
Denmark
adgivskov@hotmail.com

Andy Godfrey
Department Materials Science and
Engineering
Tsinghua University
Beijing 100084
P.R. China
awgodfrey@bigfoot.com

Carsten Gundlach
Center for Fundamental Research: Metal Structures in Four Dimensions
Materials Research Department
Risø National Laboratory
P.O. Box 49
4000 Roskilde
Denmark
carsten.gundlach@risoe.dk

Jinyu Guo
Shenyang National Laboratory for Materials Science
Institute of Metal Research
Chinese Acadamy of Sciences
Shenyang 110016
P.R. China
jyguo@imr.ac.cn

Shouzhen Guo
School of Materials Science and Engineering
University of Science and Technology Beijing
Beijing 100083
P.R. China
guoshouzhen@sohu.com

Niels Hansen
Center for Fundamental Research: Metal Structures in Four Dimensions
Materials Research Department
Risø National Laboratory
P.O. Box 49
4000 Roskilde
Denmark
niels.hansen@risoe.dk

Changshu He
School of Materials and Metallurgy
Northeastern University
PO Box 350
Shenyang 110006
P.R. China
hechsh@hotmail.com

Jing Hu
School of Materials Science and Engineering
Shanghai JiaoTong University
Shanghai
P.R. China
hujing662002@yahoo.com.cn

Zhuochao Hu
School of Materials and Metallurgy
Northeastern University
PO Box 350
Shenyang 110007
P.R. China
xiaohu_cn@163.net

Xiaoxu Huang
Center for Fundamental Research: Metal Structures in Four Dimensions
Materials Research Department
Risø National Laboratory
P.O. Box 49
4000 Roskilde
Denmark
xiaoxu.huang@risoe.dk

Thomas Jensen
Instiute of Physics and Astronomy
University of Aarhus
Ny Munkegade
8000 Aarhus
Denmark
Thomasj@ifa.au.dk

Jun Jiang
Department Materials Science and Engineering
Tsinghua University
Beijing 100084
P.R. China
Jiangjun98@mails.tsinghua.edu.cn

Haijun Jin
Shenyang National Laboratory for Materials Science
Institute of Metal Research
Chinese Acadamy of Sciences
Shenyang 110016
P.R. China
hjjin@imr.ac.cn

Dorte Juul Jensen
Center for Fundamental Research: Metal Structures in Four Dimensions
Materials Research Department
Risø National Laboratory
P.O. Box 49
4000 Roskilde
Denmark
dorte.juul.jensen@risoe.dk

Carina Jørgensen
Department of Chemistry
University of Copenhagen
Denmark
carjor@fys.ku.dk

Krysztof Kurzydłowski
Department of Materials Science and Engineering
Warsaw University of Technology
Wołoska 141
02-507 Warsaw
Poland
kjk@immat.pw.edu.pl

Axel Wright Larsen
Center for Fundamental Research: Metal Structures in Four Dimensions
Materials Research Department
Risø National Laboratory
P.O. Box 49
4000 Roskilde
Denmark
axel.wright.larsen@risoe.dk

Erik Lauridsen
Center for Fundamental Research: Metal Structures in Four Dimensions
Materials Research Department
Risø National Laboratory
P.O. Box 49
4000 Roskilde
Denmark
erik.mejdal@risoe.dk

Bolong Li
Department Materials Science and Engineering
Tsinghua University
Beijing 100084
P.R. China
leebolong99@mails.tsinghua.edu.cn

Longfei Li
School of Materials Science and Engineering
University of Science and Technology Beijing
Beijing 100083
P.R. China
llf_li@hotmail.com

Zhengjie Li
Department Materials Science and Engineering
Tsinghua University
Beijing 100084
P.R. China
lizhengjie@mails.tsinghua.edu.cn

Feng Lin
Department Materials Science and Engineering
Tsinghua University
Beijing 100084
P.R. China
linf01@mails.tsinghua.edu.cn

Gang Liu
Shenyang National Laboratory for Materials Science
Institute of Metal Research
Chinese Acadamy of Sciences
Shenyang 110016
P.R. China
Gliu@imr.ac.cn

Wei Liu
Department of Materials Science and Engineering
Tsinghua University
Beijing 100084
P.R. China
liuw@mail.tsinghua.edu.cn

Qing Liu
Department Materials Science and Engineering
Tsinghua University
Beijing 100084
P.R. China
qing.liu@tsinghua.edu.cn

Ke Lu
Shenyang National Laboratory for Materials Science
Institute of Metal Research
Chinese Acadamy of Sciences
Shenyang 110016
P.R. China
lu@imr.ac.cn

Majbritt D. Lund
Department of Geology
University of Copenhagen
Denmark
lm020278@geo.geol.ku.dk

Weimin Mao
School of Materials Science and Engineering
University of Science and Technology Beijing
Beijing 100083
P.R. China
wmmao@mater.ustb.edu.cn

Lawrence Margulies
Center for Fundamental Research: Metal Structures in Four Dimensions
Materials Research Department
Risø National Laboratory
P.O. Box 49
4000 Roskilde
Denmark
Margulie@esrt.fr

Adam Morawiec
Institute of Metallurgy and Materials Science
Polish Academy of Sciences
Reymonta 25
30-059 Krakow
Poland
nmmorawi@cyf-kr.edu.pl

Søren Fæster Nielsen
Center for Fundamental Research: Metal Structures in Four Dimensions
Materials Research Department
Risø National Laboratory
P.O. Box 49
4000 Roskilde
Denmark
soeren.faester.nielsen@risoe.dk

Jun Pang
Shenyang National Laboratory for Materials Science
Institute of Metal Research
Chinese Acadamy of Sciences
Shenyang 110016
P.R. China
jpang@imr.ac.cn

Wolfgang Pantleon
Center for Fundamental Research: Metal Structures in Four Dimensions
Materials Research Department
Risø National Laboratory
P.O. Box 49
4000 Roskilde
Denmark
wolfgang.pantleon@risoe.dk

Derek K. Pedersen
Aalborg University
9000 Aalborg
Denmark
derek_k_pedersen@hotmail.com

Jakob Haahr Petersen
Instiute of Physics and Astronomy
University of Aarhus
Ny Munkegade
8000 Aarhus
Denmark
Jakob_haahr@hotmail.com

Henning F. Poulsen
Center for Fundamental Research: Metal Structures in Four Dimensions
Materials Research Department
Risø National Laboratory
P.O. Box 49
4000 Roskilde
Denmark
henning.friis.poulsen@risoe.dk

Brian Ralph
Ty Carrog
St. Brides-Super-Ely
Cardiff
Wales
CF5-6EY
United Kingdom
brian.ralph@brunel.ac.uk

Søren Schmidt
Center for Fundamental Research: Metal Structures in Four Dimensions
Materials Research Department
Risø National Laboratory
P.O. Box 49
4000 Roskilde
Denmark
soeren.schmidt@risoe.dk

Casper Thorning
IPL, Building 204
Technical University of Denmark
DK-2800 Lyngby
Denmark
Casper.thorning@risoe.dk

Weiping Tong
Shenyang National Laboratory for Materials Science
Institute of Metal Research
Chinese Acadamy of Sciences
Shenyang 110016
P.R. China
wptong@imr.ac.cn

Ke Wang
Shenyang National Laboratory for Materials Science
Institute of Metal Research
Chinese Acadamy of Sciences
Shenyang 110016
P.R. China
sxhsx@hotmail.com

Zhenbo Wang
Shenyang National Laboratory for Materials Science
Institute of Metal Research
Chinese Acadamy of Sciences
Shenyang 110016
P.R. China
zbwang@imr.ac.cn

Grethe Winther
Center for Fundamental Research: Metal Structures in Four Dimensions
Materials Research Department
Risø National Laboratory
P.O. Box 49
4000 Roskilde
Denmark
grethe.winther@risoe.dk

Guilin Wu
Department Materials Science and Engineering
Tsinghua University
Beijing 100084
P.R. China
wuguilin99@mails.tsinghua.edu.cn

Shiding Wu
Shenyang National Laboratory for Materials Science
Institute of Metal Research
Chinese Acadamy of Sciences
Shenyang 110016
P.R. China
shdwu@imr.ac.cn

Qingfeng Xing
Center for Fundamental Research: Metal Structures in Four Dimensions
Materials Research Department
Risø National Laboratory
P.O. Box 49
4000 Roskilde
Denmark
qingfeng.xing@risoe.dk

Ping Yang
School of Materials Science and Engineering
University of Science and Technology Beijing
Beijing 100083
P.R. China
yangp@mater.ustb.edu.cn

Zhigang Yang
Department Materials Science and Engineering
Tsinghua University
Beijing 100084
P.R. China
zgyang@tsinghua.edu.cn

Mei Yao
School of Materials Science and Engineering
Yanshan University
Qinhuangdao 066004
Hebei
P.R. China

Hongwang Zhang
Shenyang National Laboratory for Materials Science
Institute of Metal Research
Chinese Acadamy of Sciences
Shenyang 110016
P.R. China
hwzhang2001@yahoo.com.cn

Jing Zhang
School of Materials Science and Engineering
Chongqing University
Chongqing 400044
P.R. China
jingzhang@cqu.edu.cn

Jinwu Zhang
School of Materials Science and Engineering
Yanshan University
Qinhuangdao 066004
Hebei
P.R. China

Yudong Zhang
School of Materials and Metallurgy
Northeastern University
PO Box 350
Shenyang 110008
P.R. China
Zhangyd_98@yahoo.com

Yuan Zhou
Department Materials Science and Engineering
Tsinghua University
Beijing 100084
P.R. China
zhouyuan@mails.tsinghua.edu.cn

Jing Zhu
Department Materials Science and Engineering
Tsinghua University
Beijing 100084
P.R. China
jzhu@tsinghua.edu.cn

Liang Zuo
School of Materials and
Metallurgy
Northeastern University
PO Box 350
Shenyang 110009
P.R. China
lzuo@mail.neu.edu.cn

Assembled participants at the Geometry of Microstructures Summer School immediately prior to the First Chinese-Danish Symposium on the Characterisation of Microstructures. Almost all of the pictures students, scientists and lecturers stayed on to attend the symposium.

Schedule

Monday 19 August

08:30 **Opening**

Deformation I

08:40 **Nanostructured metals – processing, microstructure and properties**
Niels Hansen

09:10 **Grain Refinement Process of Metals During Surface Mechanical Attrition (SMA)**
K. Lu

09:40 **The Grain Refinement Mechanism of AISI 304 Stainless Steel during Surface Mechanical Attrition (SMA)**
H. W. Zhang & K. Lu

10:00 **Orientation correlations in aluminium deformed by ECAE**
Jacob R. Bowen, Oleg. V. Mishin, Philip B. Prangnell and Dorte Juul Jensen

10:20 **SEM/ECC Investigation of Microstructural Evolution during Cyclic Deformation of Ultra-fine Grain Copper Processed by ECAP**
S. D. Wu

10:40 **Tea and Coffee Break**

Techniques I

11:10 **Combining TEM and EBSP studies in the investigation of metal deformation processes**
Q. Liu

11:30 **TEM investigations of deformation and recovery microstructures in aluminium alloys**
Claire Y. Barlow

11:50 **Change of planar structure trace direction induced by sample tilting in TEM**
Xiaoxu Huang

12:10 **TEM characterization of surface and interface structures**
Qingfeng Xing

12:30 **In-Situ TEM Observation of Crack Propagation Process of 304L Steel during Tensile Deformation**
J. W. Zhang

12:50 **Lunch**

Techniqes II

14:00 **3DXRD – a novel tool for materials science**
Henning F. Poulsen

14:30 **Structural Refinement of the individual grains in a polycrystal**
Søren Schmidt, Gavin B.M. Vaughan and Henning F. Poulsen

14:50 **A computer simulating tool for 3DXRD microscope**
Xiaowei Fu, Søren Schmidt, Henning Friis Poulsen

15:10 **Investigation on Medium Temperature Phase Transformation in AA1235 Aluminum Sheets for Foils**
J. Zhang & F. S. Pan

15:30 **Grain Boundary Design and Control and Their Applications in Fe-6.5%Si Alloy**
H. W. Song

15:50 **Tea and Coffee Break**

Deformation II

16:20 **Cold-deformed Structure in TiNi Based Shape Memory Alloy**
W. Cai & L. C. Zhao

16:40 **Preferred planes of deformation induced dislocation boundaries**
Grethe Winther

17:00 **Disorientations across deformation-induced boundaries**
Wolfgang Pantleon

17:20 **Characterization of Deformation Behaviour and Texture Formation in Magnesium Alloy AZ31 with Initial Texture**
P. Yang & G. Gottstein

17:40 **Local strain measurements by using marker particles and synchrotron X-ray absorption tomography**
Søren F. Nielsen, Felix Beckmann, Casper Thorning, John A. Wert and Henning F. Poulsen

18:00 **End of 1st Day**

18:00 **Dinner**

Tuesday 20 August

Recrystallisation

08:30 **Microstructure and texture evolution in cold-rolled interstitial-free steel sheets during high magnetic field annealing**
C. S. He, Y. D. Zhang, X. Zhao, L. Zuo, J. C. He, K. Watanabe, T. Zhang and G. Nishijima

09:00 **Stereological Studies of Recrystallization Kinetics**
Dorte Juul Jensen

09:20 **Automatic Characterization of Recrystallizing Microstructures by EBSD Line Scans**
Axel W. Larsen and Dorte Juul Jensen

09:40 **Effect of External Electric Field on Second Phase Particles and Recrystallization Texture of Deep-Drawing 08Al Killed Steel**
Zuo Lian & Zhao Xian

10:00 **Recrystallization studies using the 3DXRD microscope**
Erik M. Lauridsen, Henning F. Poulsen and Dorte Juul Jensen

10:20 **Tea and Coffee Break**

Techniques III

10:50 **Simulation of orientation mapping as a tool for improved quantitative understanding of experimental EBSP data**
Andy Godfrey

11:20 **Experimental observations of local crystal orientation distributions in strained single- and polycrystals**
Casper Thorning, John A. Wert and Xiaoxu Huang

11:40 **Experimental observation and modelling of average lattice rotations of individual grains in columnar grained nickel**
Guilin L. Wu, Grethe Winther, Qing Liu

12:00 **Elastic strain and grain rotation measurements of individual grains during polycrystalline deformation**
Lawrence Margulies

12:20 **End of symposium**

12:40 **Lunch**
Return to Beijing

TEM investigations of deformation and recovery microstructures in aluminium alloys

Claire Y. Barlow

University of Cambridge, Manufacturing Engineering, Department of Engineering, Mill Lane, Cambridge CB2 1RX, UK

The work reported here was part of a study of the evolution of microstructures in deformed aluminium alloy containing a fine distribution of alumina particles, highlighting the role of the alumina particles. The microstructures were analysed quantitatively using TEM techniques, and the results assessed in the light of the mechanical properties of the alloy.

The material was 99.5% purity aluminium powder containing 3.8 vol.% fine alumina particles from surface oxide films. It was atomised and ball-milled, then consolidated, extruded, cold rolled and finally heated for 12h at 625^{o}C. The starting material for the experiments was almost fully recrystallised with a large grain size (grains of the order of millimetres in diameter). It contained large numbers of very small alumina particles in the form of platelets, about 10nm in thickness and with diameters between 50 and 100nm. These particles were distributed non-uniformly, tending to lie in bands parallel to the working direction. The material was deformed by rolling, with the rolling direction parallel to the extrusion direction, to strains of 1.4. 2.7 and 3.5. Foils for TEM were taken from longitudinal sections (foils contained the rolling direction and the direction normal to the rolling plane). Mechanical properties were obtained from tensile tests. Subgrain wall misorientations were measured using a microdiffraction Kikuchi method.

The development of the deformation microstructure has been discussed in detail elsewhere (Barlow, Hansen and Liu 2002; Barlow and Hansen 1989). In the early stages, the dislocation density rose rapidly and the dislocations started to form cell walls (boundaries of appreciable thickness formed of loose tangles of dislocations, separating comparatively dislocation-free regions). The changes in crystallographic orientation across these walls (the misorientation) were small, less than 3º. As deformation increased the cell walls were increasingly replaced by sharp walls, which look like grain boundaries, and are termed subgrain walls. The misorientation across subgrain walls may be low or high angle (>16˚). The par-

ticular significance of high-angle boundaries in the present work is that these are able to migrate, whilst low-angle boundaries is general cannot.

It was notable that the structure developed most rapidly in regions where the particle density was highest. However, by a strain of 1.4 there was no appreciable difference in regions of different particle density. Further, it was noted that at strains below about 2.7 most alumina particles were in contact with dislocations or boundaries, indicating some pinning behaviour. At higher strains, boundaries and dislocations were increasingly unlikely to be pinned by the alumina particles.

Deformation structures in the matrix alloy without particles were very different (e.g. Barlow and Hansen 1991). The indication was that the alumina particles limited slip distances within the material, causing more rapid development of the deformation structure. Impeding the slip in this way will result in higher point-defect concentrations, as dislocations are forced to move by non-conservative slip. The particle-containing alloy also reached a stable minimum subgrain size by a strain of about 2, whilst subgrain sizes were still falling the matrix alloy. The proportion of high-angle boundaries was very high, even at the lowest strain studied, and the proportion continued to increase with strain. It was very significantly greater than in the matrix alloy.

The tensile tests demonstrated that the yield stress in the particle-containing alloy had reached a stable maximum by a rolling strain of about 1.4. Since the subgrain wall misorientations were still changing at this strain, the indication was that the yield stress was influenced by the subgrain sizes (Barlow and Hansen 1991), with wall strength variability being insignificant.

The effect of the alumina particles may be summarised as accelerating the formation and stabilisation of deformation microstructures. It is proposed that the stabilisation of the structures requires migration of high-angles grain-boundaries, and that this is enhanced by high densities of point defects.

Acknowledgements

This presentation draws on work already published together with co-authors: Barlow, Hansen and Liu (2002)

References

Barlow, C.Y. and Hansen, N. (1989). Deformation structures in aluminium containing small particles. *Acta Metall.* 37, 1313-1320.

Barlow, C.Y. and Hansen, N. (1991). Deformation structures and flow stress in aluminium containing short whiskers. *Acta Metall. Mater.* 39 1971-1979.

Barlow C. Y., Hansen, N., Liu, Y.L. (2002) Fine scale structures from deformation of aluminium containing small alumina particles. *Acta Materialia.* 50 171-182

Orientation correlations in aluminium deformed by ECAE

Jacob R. Bowen[1], Oleg. V. Mishin[1], Philip B. Prangnell[2] and Dorte Juul Jensen[1]

[1]Center for Fundamental Research: Metal Structures in Four Dimensions, Materials Research Department, Risø National Laboratory, P.O. Box 49, DK-4000 Roskilde, Denmark
[2]Manchester Materials Science Centre, UMIST, Grosvenor Street, Manchester, M1 7HS, United Kingdom

It is now well known that grain subdivision occurs during plastic deformation (Hughes and Hansen 1997). At medium to high strains, due to the formation of many new deformation induced high angle boundaries, it is no longer possible to recognise the original grain structure (Hughes and Hansen 2000). However, it has been found that in aluminium cold rolled to 50 and 90% reduction, strong correlations can exist between neighbouring orientations (Juul Jensen 1997). This was shown by comparing experimentally determined misorientation distributions measured across the individual dislocation boundaries to the corresponding theoretical misorientation distributions calculated assuming a random mixture of the orientations observed in the deformation texture. These results mean that, a memory of the original grain structure exists which strongly influences the local orientation development within a grain and thus spatial orientation correlations continue to exist in the deformation structure.

The work presented here (see Bowen, Mishin, Prangnell et al. (2002) for more information) investigates whether such orientation correlations remain after deformation to very high strains. An indication that such correlations may exist in severely deformed alloys, is that in some investigations, significantly large fractions of low angle boundaries have been found to be retained after deformation to strains as high as ten (e.g. Bowen (2000), Mishin, Juul Jensen and Hansen (2000)). In this investigation, boundary misorientation distributions have been determined in a single phase aluminium sample deformed to a strain of ten by equal channel angular extrusion (ECAE) from TEM and by high resolution electron backscattered diffraction (HR-EBSD). These two techniques have been used to ensure good statistics and good angular, as well as spatial resolution. The *experimentally measured boundary* misorientation distributions are compared to the *calculated* misorientation distributions expected if the measured orientations were randomly distributed.

Orientations obtained by both EBSD and TEM generate similar misorientation distributions despite a large difference in statistics. The calculated and experimentally measured distributions (see Figure 1.) are found to be significantly different even after a strain of ten, suggesting that the

misorientation distribution cannot be reproduced merely by randomly mixing the orientations present in the microstructure due to observed correlations, between orientations over low and high angle boundaries. The connectivity of correlated orientations may also be of importance in the interpretation of mechanical properties of materials deformed to very large strains.

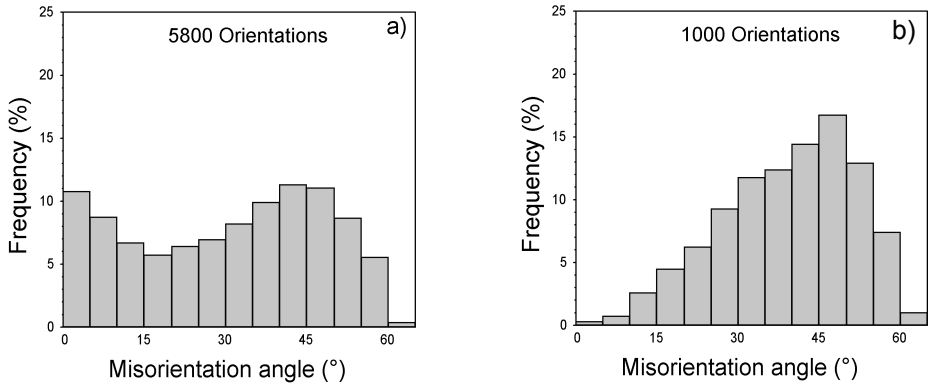

Figure 1: a) Experimentally measured boundary misorientation distribution by EBSD and b) the calculated misorientation distribution based on 1000 randomly selected orientations from the EBSD dataset.

Acknowledgements

Part of this work was supported by the Engineering Science Centre for Structural Characterisation and Modelling of Materials at the Risø National Laboratory and by Alcan International (Banbury Laboratories, UK) via the Ultra-fine Grained Alloys project at the Manchester Materials Science Centre. Dr T. J. Sabin is gratefully acknowledged for her help in the random selection of orientations.

References

Bowen, J. R. 2000 The formation of ultra-fine grained model aluminium and steel alloys. PhD Thesis. UMIST, Manchester, UK.

Bowen, J. R., Mishin, O. V., Prangnell, P. B., and Juul Jensen, D. (2002). Orientation correlations in aluminium deformed by ECAE. Scripta Materialia 47 (5), 289-294.

Hughes, D. A. and Hansen, N. (1997). High Angle Boundaries Formed by Grain Subdivision Mechanisms. Acta Materialia 45 (9), 3871-3886.

Hughes, D. A. and Hansen, N. (2000). Microstructure and Strength of Nickel at Large Strains. Acta Materialia 48 (11), 2985-3004.

Juul Jensen, D. (1997). Effects of orientation correlations on misorientation distributions in cold-deformed aluminium. Materials Science and Engineering A 234-236 762-765.

Mishin, O. V., Juul Jensen, D., and Hansen, N. (2000) Characterisation of deformation structures in ECAE processed copper. Proc. of the 21st, Risø International Symposium on Materials Science, Eds. N. Hansen, X. Huang, D. Juul Jensen, E. M. Lauridsen, T. Leffers, W. Pantleon, T. J. Sabin, and J. Wert, Denmark, 445-449.

Cold-deformed structure in TiNi based alloys

Wei Cai, Y.F. Zheng and L.C. Zhao

School of Materials Science and Engineering, Harbin Institute of Technology, Harbin 150001, P.R. China

Twinning orientation relationships are the prevailing feature of martensites, both thermally induced and stress induced, in TiNi based shape memory alloys. These glissile movements of various twinning interfaces allow the recovery of the predeformation microstructure and the macroscopic shape upon unloading or heating, which correspond to the superplasticity and shape memory effect, respectively. Thus, an understanding of the microstructural evolution with the cold deformation strain and corresponding twinning interface structures is essential.

In the present paper, the microstructural evolution and deformation micromechanism of cold-deformed TiNi based alloys, both in the martensite and parent phase conditions, have been reviewed. The emphasis is placed on the modification of the microstructure proceed through atomic migration such as the coalescence and rearrangement of martensite variants and the adjustment and development of internal twinning. The atomic configuration at the pre-existing twinning boundaries after deformation have been revealed. The corresponding deformation micromechanisms were discussed.

The TEM and HREM observations show that with the increase of the thickness reduction, the following phenomena happen in cold deformed TiNi alloys: the dominant deformation mechanism changes from the coalescence of the martensite variants to the coalescence of the substructural bands and the introduction of the secondary twinning plates; the quantities of the (100) compound and <011> Type II twinning plates are reduced, with the increase of $(11\bar{1})$ Type I, (001) compound and (011) Type I twinning bands and the introduction of (111) Type I twinning plates; The (100) intervariant boundary gradually loses its mobility and becomes wavy, the <011> Type II twinning boundary changes from the gradually and randomly curved one to the distorted one, the $(11\bar{1})$ Type I, (001) compound and (011) Type I twinning boundaries become stepped, and the (111) Type I twinning boundary exhibits wavy feature as shown in Fig.1.

Besides the ordinary slip, the adjustment and development of the internal secondary twinning from $(11\bar{1})$ Type I twin to <011> Type II /or (011) Type I twin, (111) Type I twin and (001) compound twin as shown in Fig.2, happen concurrently or in combination inside the SIM variants with the further deformation in Ti-Ni-Nb alloy. The corresponding de-

formation mechanisms include stress induced reorientation of SIM substructural bands by the most favorably oriented twin system, stress induced migration of SIM substructural boundary through internal twinning and stress induced injection of foreign SIM variant to the preexisting substructural bands.

Based on the analyses of microstructural changes with the applied stress, the intrinsic reason for the linear superelasticity of the moderately cold drawn TiNi alloy was confirmed to be associated with the appearance and disappearance of (001) microtwinning inside the <011> Type II substructural bands.

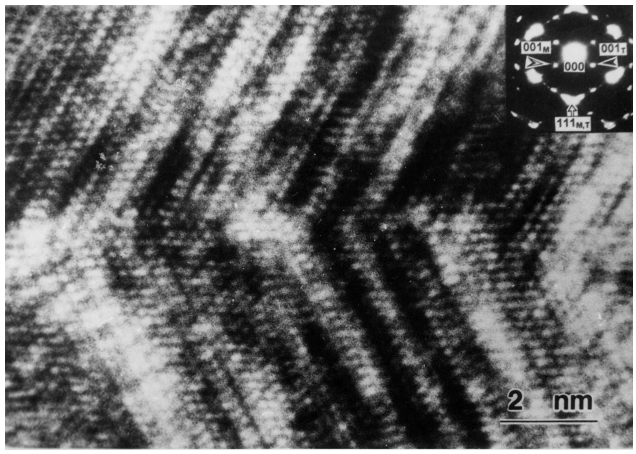

Figure 1: HREM image of (111) type I twinning boundary in the TiNi alloy specimen subjected to 22% thickness reduction

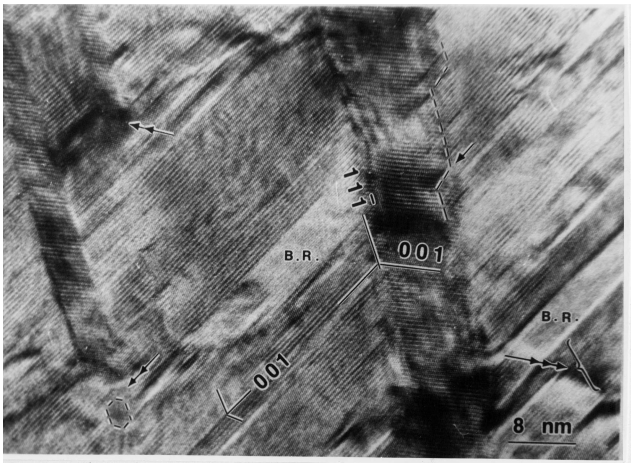

Figure 2: HREM image showing the twinning development from (11$\bar{1}$) Type I mode to (001) compound mode in the 16% deformed $Ti_{46.3}Ni_{44.7}Nb_9$ alloy specimen, electron beam // [$\bar{1}$ 10]$_{M,T.}$

A computer simulating tool for 3DXRD microscope

Xiaowei Fu, Søren Schmidt, Henning Friis Poulsen

Center for Fundamental Research: Metal Structures in Four Dimensions, Materials Research Department, Risø National Laboratory, P. O. Box 49, DK-4000 Roskilde, Denmark

A novel technique, named as 3DXRD microscopy, has recently been developed based on diffraction of high-energy X-ray (≥50 keV) at Risø, which offers the possibility of non-destructive measurement of the crystallographic orientation and time resolved three dimensional mapping of structures to the micrometer scale (Poulsen 2001). By means of the GRAINDEX indexing program, 2D grain boundary maps have been reconstructed using a kind of 3DXRD tracking method, which is proved to be successful for undeformed or weakly deformed polycrystal materials (Lauridsen 2001).

In this work, we have written a simulating tool for evaluation of a new 2D reconstruction method. In this simulator, a 2D/3D polycrystal microstructure is firstly created based on a Monte Carlo method. Each voxel within the 'sample' has been assigned an orientation. According to the experiment set-up and related X-ray diffraction theory, a set of diffraction images is generated under given parameters such as the material type, beam width, sample position, X-ray energy, detector position, mosaic spread and so forth.

The simulator has provided following functions:

- The indexing results from the GRAINDEX program can be evaluated by comparing with a set of theoretical images or diffraction spots created by simulator. Using simulated grains with mosaic spread and deformed grains, we can also test how far that GRAINDEX program will run.
- Theoretical diffraction images of grains with simple or regular shapes can be generated, which is very useful at the beginning of building the 2D/3D reconstruction model.

The indexing result from the GRAINDEX program and the new reconstruction method were tested by simulation. Figure 2 shows the reconstructed map of a grain compared with original grain map and the error is less than 1 μm. The results reveal that the both indexing of the GRAINDEX program and reconstruction method are validated accurate with the assistance of the simulating tool. The resolution of detector here is 2.33 μm in horizontal direction and 2.33 μm in vertical direction. Other testing and analysing work is still on going.

Acknowledgements

The authors gratefully acknowledge the Danish National Rearch Foundation for supporting the Center for Fundamental Rearch: Metal Structures in Four Dimensions, within wihich this work was performed.

References

Poulsen, H. F., Nielsen, S. F., Lauridsen, E. M., Schmidt, S., Suter, R. M., Lienert, U., Margulies, L., Lorentzen, T. and Juul Jensen, D. (2001), Three-dimensional maps of grain boundaries and the stress state of individual grins in polycrystals and powders. J. Appl. Cryst. 34 (6), 751-756.

Lauridsen, E. M., Schmidt, S., Poulsen, H.F. and Suter, R.M. (2001). Tracking: a method for structural characterization of grains in powders or polycrystals. J. Appl. Cryst. 34 (6), 744-750.

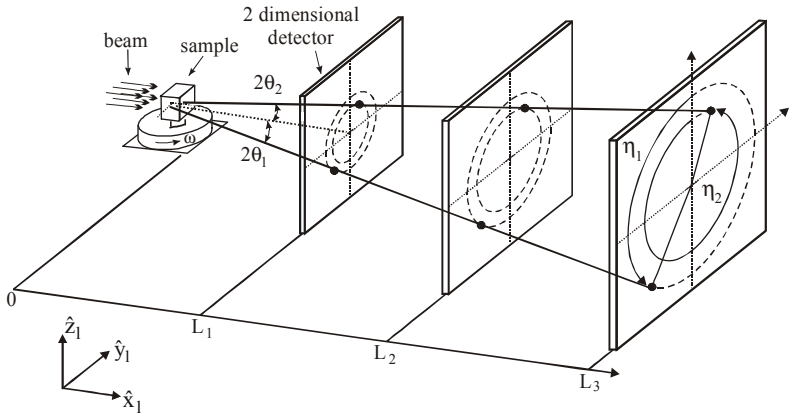

Figure 1. Sketch of the experiment set-up, including definition of angles 2θ (Bragg angle), ω (sample rotation) and η (azimuthal angle) around Debye-Scherrer cones

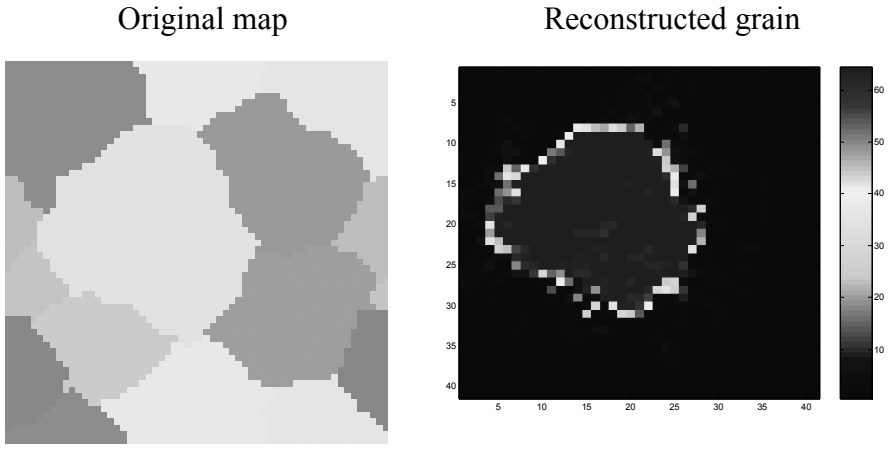

Figure 2. Validation of reconstruction method on simulated data.

Simulation of orientation mapping as a tool for improved quantitative understanding of EBSP data

Andy Godfrey

Department of Materials Science and Engineering, Tsinghua University, Beijing 100084, P.R. China

The rapid acquisition of large amounts of spatially resolved orientation data has led to the increasing use of electron back-scatter pattern (EBSP) analysis for a wide range of materials problems. There are however still some limitations to the use of the technique, arising both from the limited spatial resolution, resulting in non-indexable patterns, and from the angular resolution, resulting in an orientation noise superposed on the EBSP data. For many situations these resolution limits do not present a problem, but when the structures investigated are very fine or contain low angle misorientations, as for example for deformation microstructures, the resolution limits of the EBSP technique can seriously reduce the data quality (Huang and Juul Jensen 2000). Consequently post-processing of the data is required to maximize the information available.

By taking orientation maps (either from transmission electron microscopy or idealized configurations) EBSP data can be simulated by convoluting the maps according to the spatial and angular resolution functions. These simulated EBSP data can then be used to test the efficiency and accuracy of various post-processing techniques, comparing the results with the original, fully known, maps. Simulations can also be used to examine the effect of the user chosen map step-size on the EBSP data set.

An important parameter for the simulations is the extent of orientation noise arising from the angular resolution of the EBSP technique. The orientation noise function is straightforward to determine for single crystal (or large grain fully annealed) samples, but can not be measured directly for deformed samples, where the noise is expected to be larger. Some methods for estimating the noise on deformed samples are suggested. Whilst each method has certain limitations, the results suggest that orientation noise is significantly larger than measured on single crystal samples.

Simulations on idealised microstructures reveal that the ability of the modified Kuwahara filter (Humphreys, Bate and Hurley 2001) to improve the data resolution without the introduction of spurious artifacts depends directly on the orientation noise level in the original data (Figure 1). The presence of real boundaries in the structure also leads to further errors in the filtered data. To overcome this problem a further modification to the Kuwahara filter has been developed leading to better preserva-

tion of the true structure at triple junctions. Nevertheless, when the orientation noise level is similar to the real boundary misorientations, some distortion of the structure remains (Figure 2). Simulations of EBSP data using TEM orientation maps of low strain deformation microstructures can help to reveal the extent of information that may be available at any given EBSP map step size.

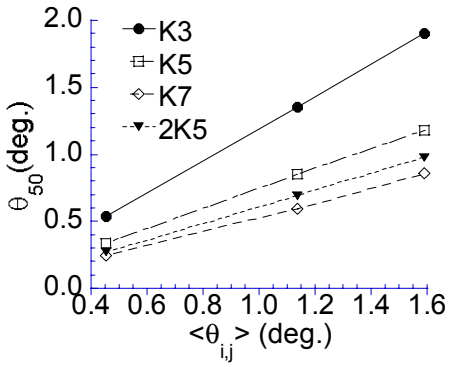

Figure 1: Simulated single crystal data. Orientation map misorientation level leaving 50 segments due to noise (θ_{50}) as a function of the initial data orientation noise level ($<\theta_{i,j}>$) for different size passes of a Kuwahara filter (K3=3x3, K5=5x5, K7=7x7, 2K5=two passes of 5x5).

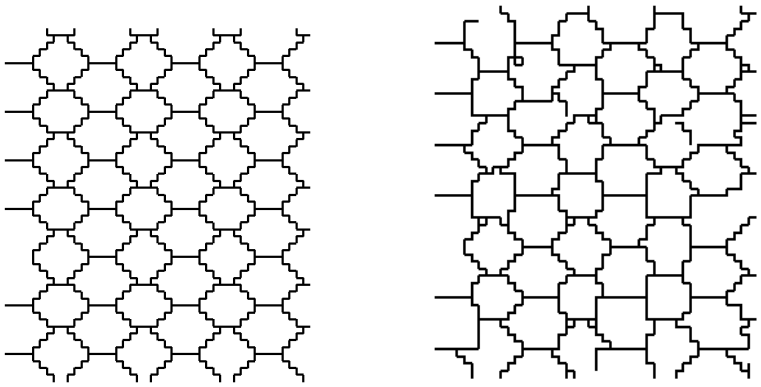

(a) (b)

Figure 2: Orientation maps (misorientation level 0.35°) for simulated low angle boundary structure ($<\theta_{bdry.}>=1.1^{o}$); (a) real structure, (b) with orientation noise ($<\theta_{i,j}>=0.44^{o}$) added and after application of the further modified Kuwahara filter.

References

Huang, X., and Juul Jensen, D. (2000) EBSD contra TEM characterisation of a deformed aluminium single crystal. Chapter 12, Electron Backscatter Diffraction in Materials Science, Eds. A. J. Schwartz, M. Kumar and B. L. Adams, Kluwer Academic, New York.

Humphreys, F. J., Bate, P., and Hurley, P. (2001). Orientation averaging of EBSD data. J. Microsc. 36, 3833-3854.

Nanostructured metals – processing, microstructure and properties

Niels Hansen

Center for Fundamental Research: Metal Structures in Four Dimensions, Materials Research Department, Risø National Laboratory, P. O. Box 49, DK-4000 Roskilde, Denmark

Nanostructured metals and alloys are of current interest and a fairly extensive literature describes processing (synthesis) and properties at such materials (e.g. Shaw, 2000, Ultrafine Grained Materials, 2000, Science of Metallic and Nanocrystallised Alloys, 2001, Mechanical Properties and Deformation Behaviour of Material having Ultrafine Microstructure, 1993). As for other materials, it is important also to study correlations between processing and structure (microstructure and texture) on one side and between structure and properties on the other. Only thereby is it possible to systematically optimise the materials. To obtain such correlations, the structure must be characterised both qualitatively and quantitatively i.e. structural parameters must be defined and determined. Such parameters are commonly process-related and as many processes have been developed (Shaw 2000), this paper shall concentrate only on one group of nanostructured materials, namely those, which are processed by plastic deformation. A number of conventional and new processes are available but common to all is the evolution of a deformation microstructure, subdivided by dislocation boundaries and grain boundaries.

The subdivision of crystals and grains during plastic deformation takes place on a macroscopic (or grain) scale into deformation bands and on a smaller scale into cellblocks and cells. This evolution is described in recent reviews (Hansen and Juul Jensen 1999, Hansen 2001). The structure refines with increasing strain and the misorientation angle across the dislocation boundaries increases in such a way that the structure at large strain is subdivided by dislocation boundaries and by high angle boundaries. The latter are the original grain boundaries supplemented by a large number of deformation induced high angle boundaries. The structural refinement at increasing strain has lead to an exploration of various deformation modes by which very large strains can be introduced into bulk materials without changing the sample shape during processing. Examples of such processes are accumulative roll bounding (ARB), cyclic extrusion compression (CEC) and equal channel angular extrusion (ECAE). The structural refinement obtained shows that the effect of strain is not very pronounced. At present, the most promising route for grain refinement appears to high-pressure torsion where it in nickel has been possible to reduce the boundary spacing to about 100 nm by applying a large shear strain. Further refinement by deformation is, however, possible,

which is demonstrated in friction where boundary spacing is low, as 10 nm has been observed. Introduction of a second phase may also lead to significant refinement as shown by cold drawing of some eutectic alloys. Turning to another structural parameter, the misorientation angle across boundaries, a pronounced effect of strain is observed as not only the average angle across boundaries increases with the strain, but also the fraction of deformation induced high angle boundaries (>15^o). This fraction may be as high as 70-80% at large strains, however significantly smaller than observed in polycrystalline specimens obtained by deformation and recrystallisation.

A typical deformation microstructure is subdivided by boundaries varying from low angle boundaries to grain boundaries and between these boundaries, the material contains a certain concentration of dislocation present as loose dislocations and as dislocation tangles. This concentration is normally not very high and if neglected, the following relationship is suggested (Hughes and Hansen, 2000):

$$\sigma = M\alpha bG\sqrt{\frac{3\theta}{bd}} + K_{HP}\cdot\frac{1}{\sqrt{D}}$$

where M is the Taylor factor and α is a number about 0.24. In this equation, the first contribution relates to low angle boundaries and the second contribution to medium and high angle boundaries. Two examples of the application of this equation will be given illustrating the behaviour of aluminium and nickel, respectively.

The processing of nanostructured metals and alloys by plastic deformation shows that the structural evolution with increasing strain follows almost the same pattern for a variety of processes. A basis, therefore, exists for the development of metals with a microstructure down to the nanometer range. However, the theoretical basis for the extrapolation has still to be formulated.

References

Shaw, L.L., Processing Nanostructured Materials. An overview, Journal of Materials, Dec. 2000, 41.

Ultrafine Grained Materials, Edited by R.S. Mishra, S.L., Semiatin, C.

Suryanarayana, N.N. Thadhani and T.C. Lowe. The Minerals, Metals and Materials Society, 2000.

Science of Metalstable and Monocrystalline Alloys-Structure, Properties and Modelling, Proc. of 22nd Risø International Symposiumon Materials Science, Risø National Laboratory, Roskilde, 2001.

Mechanical Properties and Deformation Behaviour of Material Having

Ultrafine Microstructure. Edited by M. Nastasi, D.M. Parkin and H. Gleiter, Nato ASI Series, Vol. 233. Kluwer Academic Publishers, London, 1993.

Hansen, N. and Juul Jensen, D. (1999) Phil. Trans. R. Soc. Lond. A, 357, 1447.

Hansen, N. (2001), Metall. Mater. Trans. A., 32A, 2917.

Hughes, A. and Hansen, N., Acta Mater. (2000), 48, 2985.

Microstructure and texture evolution in cold-rolled interstitial-free steel sheets during high magnetic field annealing

C. S. He[1], Y. D. Zhang[1], X. Zhao[1], L. Zuo[1], J. C. He[1], K. Watanabe[2], T. Zhang[2] and G. Nishijima[2]

[1]School of Materials and Metallurgy, Northeastern University, PO Box 350, Shenyang 110006, P.R. China
[2]Institute for Materials Research, Tohoku University, Sendai 980-8577, Japan

Over the past decades, several studies were made on the effects of magnetic annealing on the development of recrystallization and recrystallization texture in ferromagnetic or soft magnetic materials, which showed the magnetic field annealing retards the recrystallization and promotes the evolution of {100} texture components. In recent years, with the introduction of cryocooling techniques, high magnetic fields of more than 10T have become available at reasonable cost in the laboratory. In the present work, high magnetic fields were applied during annealing of cold-worked IF steel sheet for the purpose of examining the effects of high magnetic field on the development of microstructure and texture during recrystallization.

Longitudinal specimens were taken form cold-rolled IF deep drawing steel sheet of 1mm thickness. Annealing was carried out in a furnace installed in a cryocooler cooled superconducting magnet capable of generating a high magnetic field of 11T. Isothermal annealing at temperatures ranging from 650°C to 850°C was performed in a magnetic field with maximum strength of 10T with the rolling direction parallel to direction of the applied field. For comparison, equivalent cold rolled specimens were subjected to same heat treatments without the application of a magnetic field. For each specimen, three incomplete {110}, {200} and {211} pole figures were measured up to a maximal polar angle of 70° by using the Schulz back-reflection method and the Co-K_α radiation. The corresponding ODFs were calculated with the two-step method and the results were presented in terms of constant φ sections (Roe's notation). The microstructures of the specimens were examined with an optical microscope.

Microhardness measurements and microstructure observations clearly showed that the recrystallization was strongly retarded by the application of a high magnetic field during annealing. The reason for the retardation of recrystallization might be attributed to the realignment of domain

walls in the applied magnetic field, which can act as a barrier to grain boundary migration. Consequently, the magnetic field may lower the mobility of the grain boundaries, leading to a retardation of recrystallization (fig. 1, fig. 2). Based on an ODF analysis, it was found that the {100}<100> texture component, a component of α-fiber (RD//<110>) texture, was intensified by the magnetic field annealing at 650°C for 25min. With increase of annealing temperature, specimens annealed both with and without magnetic field exhibited the same tendency of texture development, namely an enhancement of γ-fiber (ND//<111>) and a weakening of the α-fiber. However the development of the recrystallization γ-fiber texture and the decrease of {100}<110> texture component were both retarded by the applied high magnetic field.

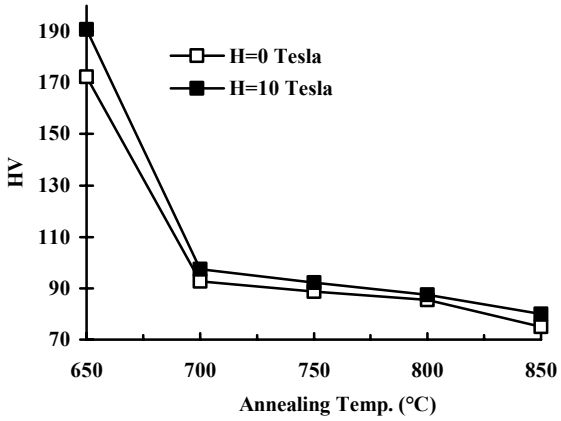

Fig.1 Microhardness vs annealing temperature

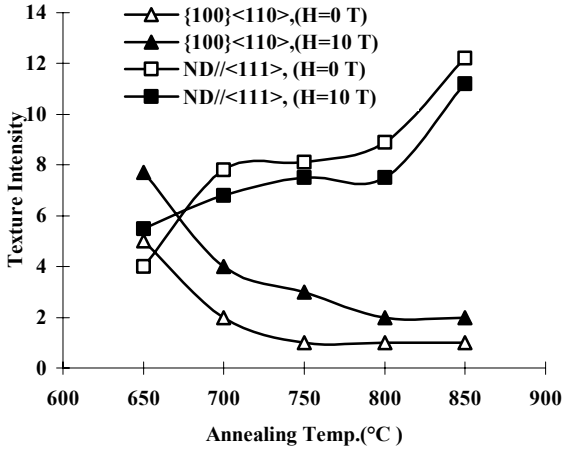

Fig.2 Texture intensity vs annealing temperature

Change of planar structure trace direction induced by sample tilting in TEM

Xiaoxu Huang

Center for Fundamental Research: Metal Structures in Four Dimensions, Materials Research Department, Risø National Laboratory, P. O. Box 49, DK-4000 Roskilde, Denmark

A planar structure intersects with a sample surface and forms a straight intersecting line, i.e., a trace, on the surface. When observing this trace in TEM, the projected trace direction changes with sample tilting. This tilting effect on the trace direction is well known as a main source of the inaccuracy in identification of crystallographic planes of planar structures based on trace analysis. Therefore, it is important to analyze the dependence of the trace direction change on tilting angle. In this work, such an analysis is made in terms of a double-tilt sample holder.

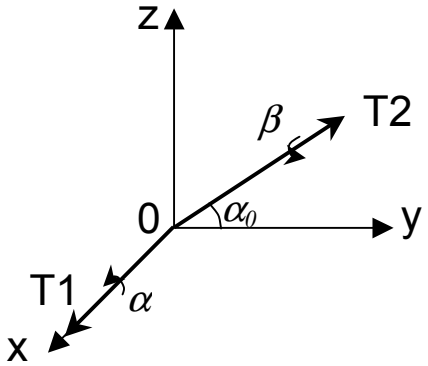

Figure 1. Geometrical relationship between the two axes of a double-tilt sample holder and a fixed orthogonal coordinate system xyz.

Fig 1 shows the geometrical relationship between a fixed reference orthogonal coordinate system, xyz, and the two tilt axes, T_1 and T_2, of a double-tilt holder. The x-axis coincides with the first tilt axis T_1 (i.e., the longitudinal axis of the holder), while the z-axis is parallel to the optical axis of the microscope. The second tilt axis T_2 of the holder lies in the yz-plane, and its exact position depends on the tilt angle (α_0) of the first tilt axis T_1. Two matrices that describe the change of a vector of the specimen in the fixed orthogonal system when the specimen is tilted have been established (Liu, Meng and Hong, 1989). In terms of these matrices, an equation for determining the correlation of the trace directions at two arbitrary tilt positions (α_1 β_1) and (α_2 β_2) can be deduced as

$$\psi_2 = \arctan\left[\left(\frac{\tan\psi_1 \cos\beta_1}{\cos\alpha_1} - \tan\alpha_1 \sin\beta_1\right) + \tan\alpha_2 \sin\beta_2\right]\frac{\cos\alpha_2}{\cos\beta_2} \qquad (1)$$

where ψ_1 and ψ_2 are the trace directions at the tilt positions (α_1, β_1) and (α_2, β_2), respectively, which are described by the angles between the x-axis and traces at the corresponding tilt positions. It is seen that the final trace direction (ψ_2) depends on the tilt positions (α_1, β_1) and (α_2, β_2) before and after tilting and the initial trace direction (ψ_1). The equation can be simplified in several special cases, as discussed below.

Case 1. $\alpha_1=\beta_1=0$. Eq.(1) is simplified as

$$\psi_2 = \arctan\left(\frac{\cos\alpha_2}{\cos\beta_2}\tan\psi_1 + \sin\alpha_2 \tan\beta_2\right) \qquad (2)$$

This is a case where the sample is tilted from the zero tilt position at which the trace direction is known. This case has been discussed by Liu (1994).

Case 2. $\alpha_2=\beta_2=0$. Eq. (1) is simplified as

$$\psi_2 = \arctan\left(\frac{\cos\alpha_1}{\cos\beta_1}\tan\psi_1 - \sin\beta_1 \tan\alpha_1\right) \qquad (3)$$

This is a case where the trace direction measured at a tilted position requires transformation into that corresponding to zero tilt. This case has been discussed by Huang and Liu (1998).

Case 3. $\beta_1=\beta_2=0$. Eq.(1) is simplified as

$$\psi_2 = \arctan\left(\frac{\cos\alpha_2}{\cos\alpha_1}\tan\psi_1\right) \qquad (4)$$

This is the case for the single tilt holder.

References

Huang X. and Liu Q., (1998). Determination of crystallographic and macroscopic orientation of planar structures in TEM, Ultramicroscopy, 74, 123-130.

Liu Q., (1994). A new method for determining the normals to planar structures and their trace directions in transmission electron microscopy, J. Appl. Cryst., 27, 762-766.

Liu Q., Meng Q. C. and Hong B., (1989). Calculation of tilt angles for crystal specimen orientation adjustment using double-tilt and tilt-rotate holders, Micron and Microscopica Acta, 20, 255-259.

Stereological Studies of Recrystallization Kinetics

Dorte Juul Jensen

Center for Fundamental Research: Metal Structures in Four Dimensions, Materials Research Department, Risø National Laboratory, P. O. Box 49, DK-4000 Roskilde, Denmark

Stereology is an efficient tool for statistical studies of recrystallization kinetics based on traditional microscopy techniques: The process of recrystallization is observed on prepared internal surfaces cut from the bulk of a series of specimens being heat treated to various fractions of recrystallization, and critical microstructural properties are determined stereologically. The following microstructural properties are typically determined:

V_v, the volume fraction is recrystallized,

S_v, the interfacial area (grain boundary) density separating recrystallizing grains from deformed volumes,

$\langle\lambda\rangle$, the mean recrystallizing grain free length.

This determination is often done by a lineal analysis of the microstructure. With random test lines, V_v is equal to the line fraction of recrystallized material and $\langle\lambda\rangle$ is the mean length of all grains sectioned by the test lines. The property S_v is determined from a count of the number N_L of intersections between deformed and recrystallised material per unit length of test line as

$$S_v = 2 \cdot N_L$$

If the electron back-scattering pattern technique is used for the determination of V_v, S_v and $\langle\lambda\rangle$, the crystallographic orientation of the recrystallizing grains may be incorporated in the analysis, such that the three properties are determined for grains of different orientations, for example, for cube oriented grains. For information on this, see Juul Jensen (1997).

The three microstructural properties may be used for estimation of boundary migration rates during the recrystallization growth. A plot of $\langle\lambda\rangle$ versus annealing time is the simplest. An example including orientations is shown in Fig. 1. Here it can be seen that cube grains grow to become the largest among the recrystallizing grains. Based on such results, it is tempting to conclude that this is because the cube grains grow faster. This is, however, not necessarily so; the sizes of the grains also depend on their spatial distribution and thus on the impingement between grains, which may vary between orientation classes.

A better way to determine migration rates is based on the other two properties V_v, S_v as shown by Cahn and Hagel (Cahn and Hagel 1962),

$$\frac{dV_V}{dt} = \langle G \rangle S_V$$

where $\langle G \rangle$ is the average growth rate. This method may also be extended to include crystallographic orientations (Juul Jensen 1997). An example of such a determination is given in Figure 2. This result shows unambiguously that cube grains grow faster than the other grains in the selected example.

The microstructural properties may also be used for a fuller analysis of the recrystallization using the microstructural path concept (Vandermeer 1995). This gives information about nucleation as well as growth. Here all three properties are compared to master curves for typical nucleation and growth conditions and fitting routines are applied to find the best match. Thereby, models for the recrystallization can be found (Vandermeer and Juul Jensen 2001).

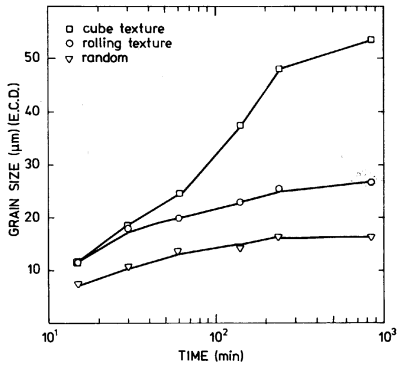

Figure 1: Plot of ⟨λ⟩ versus annealing time in commercially pure aluminium cold rolled 90% and annealed at 253°C (Juul Jensen 1997).

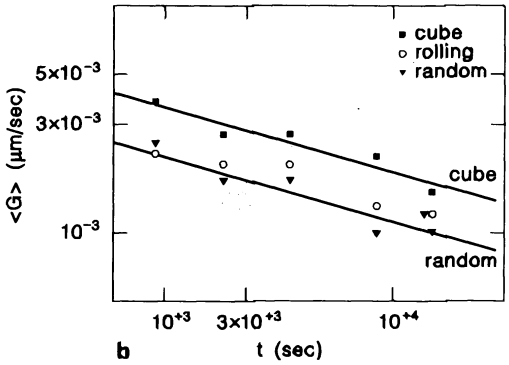

Figure 2: Average growth rates as a versus annealing time in commercially pure aluminium cold rolled 90% and annealed at 253°C (Juul Jensen 1997).

References

Juul Jensen D. (1997). Orientation aspects of growth during recrystallization. Risø Report R-978 (EN).

Cahn J. W. and Hagel W. C. (1962). Theory of the pearlite reaction.Decomposition of Austenite. Eds. V. F. Zackay and H. I. Aaronson. Interscience, 131-196.

Vandermeer R. A. (1995). Analytical modelling of recrystallization.Proc. 16th Risø Int. Symp. Eds. N. Hansen et al. Risø, 193-213.

Vandermeer R. A. and Juul Jensen D. (2001). Acta Mater 49, 2083-2094.

Automatic Characterization of Recrystallizing Microstructures by EBSD Line Scans

Axel W. Larsen and Dorte Juul Jensen

Center for Fundamental Research: Metal Structures in Four Dimensions, Materials Research Department, Risø National Laboratory, P. O. Box 49, DK-4000 Roskilde, Denmark

In the characterization of microstructures it is often important to determine the parameters (Kurzydlowski and Ralph 1995):

V_V, the volume fraction of recrystallized material,
S_V, the interfacial area (grain boundary) density separating recrystallized grains from deformed volumes,
$<\lambda>$, the mean grain intercept length.

An efficient way of determining these parameters is by *line scans* through the structure, where V_V and S_V can be determined by the linear-intercept method from stereology, which yields the following formulae (Juul Jensen 1997):

$$V_V \equiv \frac{V_{rex}}{V} = \frac{l_{rex}}{L} \ , \ S_V = \frac{2 \cdot n_{\text{int}}}{L} \ , < \lambda >= \sum_{i=1}^{N} \frac{\lambda_i}{N}$$

where V_{rex} and V are the recrystallized and total volume; l_{rex} and L are the recrystallized and total line length; and n_{int} is the number of interfaces between recrystallized and deformed material the line passes over.

A previous technique based on only *one* line was found to yield a precise determination of V_V, but S_V was typically an order of magnitude off (Krieger Lassen 2001).

A new technique has been invisaged. It is a quasi-line scans consisting of 3 parallel lines of equal length and with a mutual distance equal to the line scan step size. The central line is used for determining V_V and S_V, while the upper and lower auxiliary lines function as guides for the central line. This method has the advantages of lines scans (short measuring time and good statistics), while making use of the principle of connectivity to avoid errors (Krieger Lassen and Juul Jensen 1999).

The routine takes into account: 'bad' points (ie. data points with too few indexed Kikuchi bands), which it attempts to repair; the fact that recrystallized grains always have at least one high angle boundary; a small grain length cutoff; and gives the texture of the recrystallized grains.

It works as a series of iterations: First the it scans through all the data points on the central line, which are checked for equivalence with all its neighbors (see figure 1). The data points are then grouped into grains, 'bad' points, or deformed material depending on how many equivalent

points a data point has. Secondly, 'bad' data points are given the most representative orientation amongst its neighbors, giving a data set consisting only of grains and deformed areas. Thirdly, the first iteration is repeated and the individual grains are identified. The 4th and 5th iterations neglect grains without any high angle boundaries or grains that have a length below the user specified limit. The data set is then used to calculate the statistical and textural data.

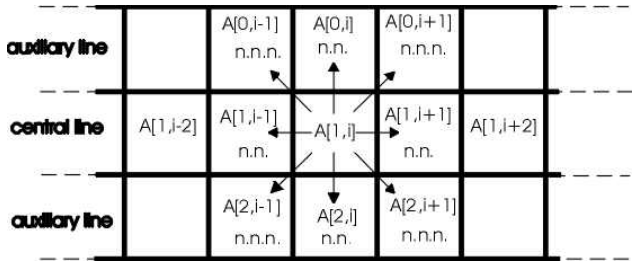

Figure 1: For every data point on the line, all neighboring data points are checked for equivalence (ie. misorientation < 0.75°). Only data points on the line contribute to the statistics.

The routine was successfully tested on three short (200 steps) line scans, which can be seen on figure 2. Normal line scans generally have lengths of order 2000+ steps.

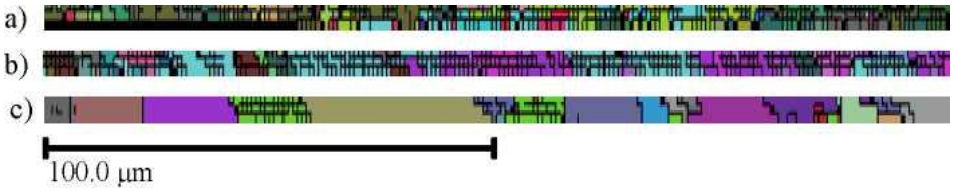

Figure 2. Orientation plots of three 3x200 µm data set with different annealing times. Misorientations with θ > 0.75° are marked with black lines. The plots are stretched vertically to make the pixels easier to see. Annealing time: a) 300 sec; b) 2000 sec; and c) 28000 sec.

References

Juul Jensen D. (1997). Orientation aspects of growth during recrystallization, Risø National Laboratory, Denmark.

Krieger Lassen N. C. (2001). Private communication.

Krieger Lassen N. C. and Juul Jensen D. (1999). Automatic recognition of recrystallized grains in partly recrystallized samples from crystal orientation maps. Proceedings of the Twelfth Conference on Textures of Materials, Szpunar J. A., NRC Research Press, Montreal (CA), Vol. 2, pages 854 to 859.

Kurzydlowski K. J. and Ralph B. (1995). The quantitative description of the microstructure of materials, CRC Press.

Recrystallization studies using the 3DXRD microscope

Erik M. Lauridsen, Henning F. Poulsen and Dorte Juul Jensen

Center for Fundamental Research: Metal Structures in Four Dimensions, Materials Research Department, Risø National Laboratory, P. O. Box 49, DK-4000 Roskilde, Denmark

A new technique is presented which allows in-situ measurements of nucleation and growth kinetics in polycrystalline materials. The technique is implemented at the 3D X-ray Diffraction (3DXRD) Microscope recently installed at the Materials Science beamline at the European Synchrotron Radiation Facility (ESRF) in Grenoble, France.

True bulk measurements are ensured by the use of focused high energy x-rays (40-100 keV) with a penetration depth of up to 4 cm in aluminium. During annealing of the sample the diffracted intensities are monitored on a 2-dimensional detector. Volumes of individual nuclei or grains are then calculated from the diffracted intensities. The kinetics of several hundred individual nuclei/grains are determined simultaneously with a time resolution of less than a minute. An intrinsic feature of the technique is that the orientation of the individual nuclei/grains is directly determined. Hence, not only can overall kinetics be studied but also orientation dependencies of the recrystallization kinetics are revealed (Lauridsen, Lienert, Juul Jensen and Poulsen 2000).

An example of use results obtained from in-situ investigation of the recrystallization kinetics of a 90% cold-rolled commercial purity aluminium alloy (AA1050) [2] is presented. In total the growth curves and crystallographic orientation of 244 individual grains were analysed, resulting in 14 cube grains, 124 grains belonging to the so-called rolling texture components, and 106 grains having random orientations. The dynamics of 5 grains having the cube orientation are shown in fig. 2. (Lauridsen, Schmidt, Margulies, Poulsen and Juul Jensen 2001).

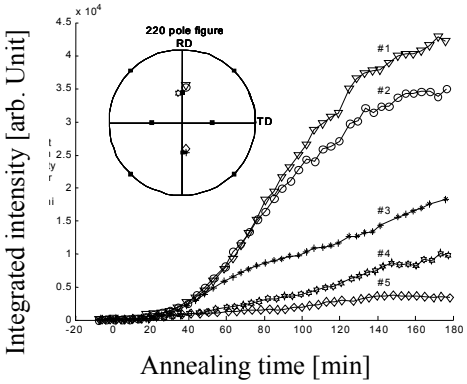

Figure 1. Growth curves for 5 grains with an orientation less than 10° degrees away from the ideal Cube orientation. The integrated intensity (in arb. units) is shown as function of annealing time. Insert: Pole figure co-ordinates of the 5 grains. (The ideal cube component is marked with ■).

From each of the 244 growth curves fundamental recrystallization parameters such as the nucleation time, the initial growth rate and the final grain size can be determined. As an example, the distribution of nucleation times, classified with respect to the three texture components, is shown in fig. 2.

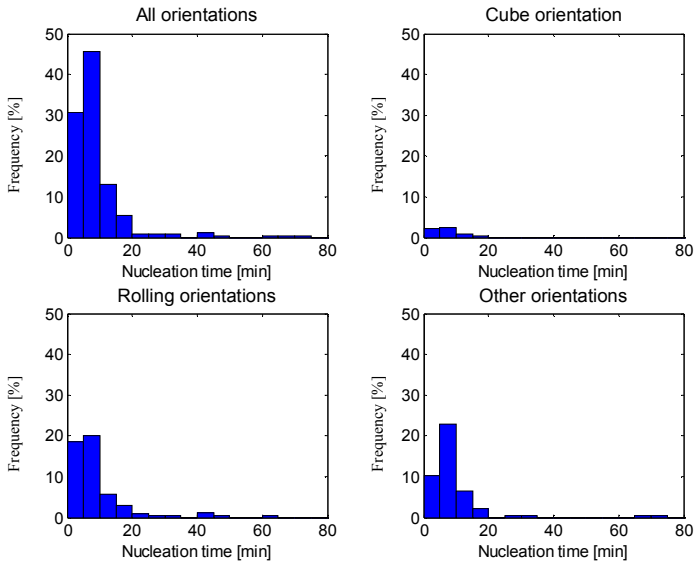

Figure 2: Histograms of nucleation times (in minutes). The frequencies based on all grains is shown in the upper, left corner. Next, the grains are sorted into three texture groups; cube, rolling and other. The respective fractional frequencies are shown.

Acknowledgements

This work was supported by the Danish Natural Research Foundation through the "Center for Fundamental Research: Metal Structures in Four Dimensions" and by the Danish Natural Science Research Council via Dansync.

References

E.M. Lauridsen, U. Lienert, D. Juul Jensen, and H.F. Poulsen (2000). Kinetics of Individual Grains During Recrystallization, Scripta Mater., 43, 561-566.

E.M. Lauridsen, S. Schmidt, L. Margulies, H.F. Poulsen and D. Juul Jensen (2001). Growth Kinetics of Individual Cube Grains as Studied by the 3D X-Ray Diffraction Microscope. Proc. of the 1st Int. Conf. on Recrystallization and Grain Growth, Editors. G. Gottstein and D.A. Molodov, Springer, Aachen, 589-594.

D. Juul Jensen, E.M. Lauridsen, R.A. Vandermeer (2002). In-Situ Determination of Grain Boundary Migration During Recrystallization. Science & Technology of Interfaces, Editors. S. Ankem, C.S. Pande, I. Ovid'ko and S. Ranganathan, TMS, Seattle, 361-374.

Combining TEM and EBSP studies in the investigation of metal deformation processes

Qing Liu

Department of Materials Science and Engineering, Tsinghua University, Beijing 100084, P.R. China

Detailed study of deformation microstructures has in the past been carried out in the transmission electron microscope (TEM), where extensive studies have shown that grain subdivision over several length scales occurs by formation of dislocation boundaries. These dislocation boundaries are predominantly rotation boundaries, and hence an important parameter to characterize is the rotation across them. A semi-automatic technique for orientation measurement has been developed (Liu 1995), allowing up to 60 measurements per hour. In contrast the EBSP technique can measure more than 10000 orientations per hour, but the spatial and angular resolution of the technique lower than in the TEM. The EBSP technique however allows the investigation of much larger sample areas than in the TEM. It is therefore of interest to try and combine TEM and EBSP studies in order the subdivision processes occurring during deformation in as much detail as possible over several length scales. Two examples of such studies are described here.

During rolling deformation single crystals of the {001}<110> a macroscopic breakup across the sample thickness is observed. Coarse step size EBSP measurements across the samples shows a pattern of matrix (uniform orientation), transtion (continuously varying orientation) and sharply alternating regions. The microstructure in the central region (with sharply alternating orientations) was investigated both using TEM and high resolution EBSP. Good agreement between measurements of several important microstructural parameters was obtained, including average dislocation wall spacing. On the basis of this, the local microstructure in the matrix and transition regions was studied by EBSP only. It was observed that in each matrix region only one set of dislocation walls was present. In the transition regions a continuous change in the dislocation cell size w seen, with the largest dislocation cells with orientations only rotated slightly from the initial orientation.

Another way to combine EBSP and TEM studies is to use the EBSP technique to improve the statistics. A detailed study of microstructural evolution of polycrystalline Al during heavily deformation was carried out in both TEM (with a semi-automatic technique) and SEM (with automatic EBSP technique). Figure 2 shows an example which indicates that a reasonably good agreement of dislocation boundary morphology

and the statistic results of the misorientations across the boundaries was obtained. Therefore, in many cases the EBSP technique can be used to assist in the characterization of microstructural evolution of materials during heavy deformation.

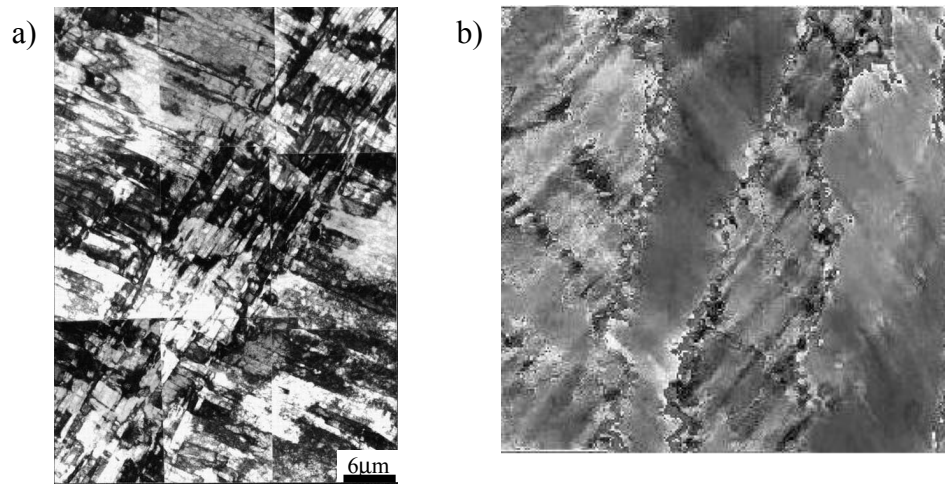

Figure 1: Example microstructures in central region of deformed single crystal as seen by TEM (a) and EBSP (b)

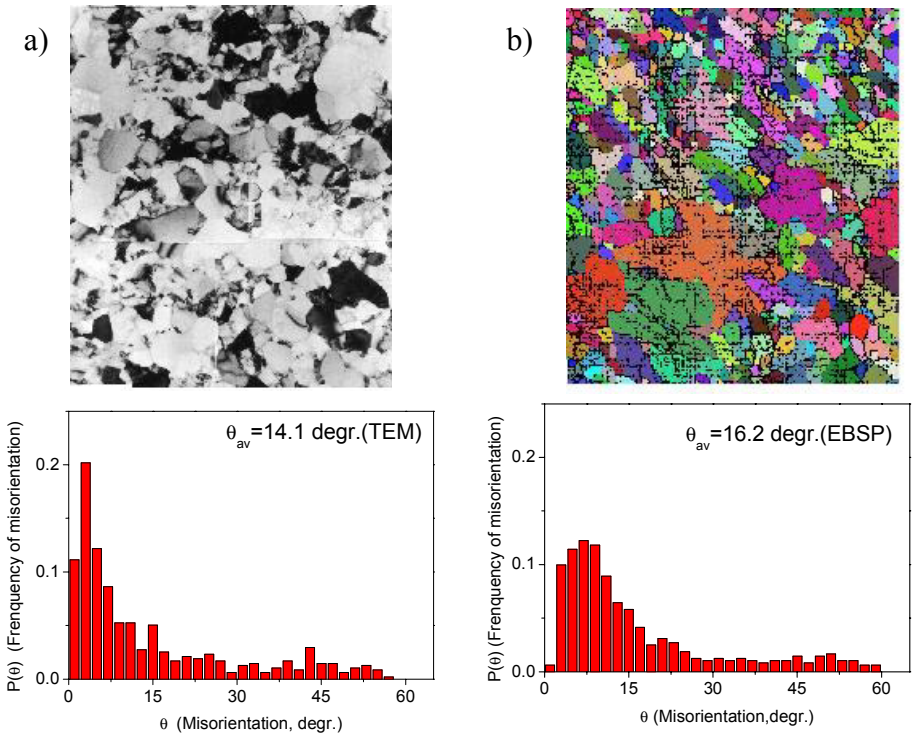

Figure 2 Statistical comparison of EBSP and TEM techniques for investigation of an ECAE deformed sample; (a) typical microstructures, (b) example misorientation distributions.

References

Liu, Q. (1995). A simple and quick method for determining orientations and misorientations of crystalline specimens in the TEM. Ultramicroscopy 60, 81-89.

Grain refinement process of metals during surface mechanical attrition (SMA)

Ke Lu

Shenyang National Laboratory for Materials Science, Institute of Metal Research, Chinese Academy of Sciences, Shenyang 110016, P.R. China

A surface mechanical attrition (SMA) treatment to metallic materials leads to formation of a nanostructured surface layer (up to 50 μm thick). This nanostructured surface layer enables the overall properties of the material to be significantly improved. The SMA processing technique has been successfully applied to several kinds of metallic materials including pure metals and engineering alloys. In this work, the grain refinement mechanism during the SMA processing was investigated in several different specimens (Fe, Cu, and AISI 304 stainless steel) by using various microstructural analysis techniques including transmission electron microscopy (TEM), scanning electron microscopy (SEM), and X-ray diffraction (XRD). The cross-sectional TEM images revealed varying microstructure characteristics at different depths from the top surface, and therefore with different strains and strain rates. It was found that the grain refinement mechanisms during SMA process, that are very different depending upon the nature of metals, may involve activities of dislocations and twins, formation of subgrain boundaries and eventually large angle grain boundaries. The grain refinement mechanism during SMA of bulk metals is closely relevant to that in other mechanical attrition processes (such as ball-milling) and severe plastic deformation processes.

Elastic strain and grain rotation measurements of individual grains during polycrystalline deformation

Lawrence Margulies

Center for Fundamental Research: Metal Structures in Four Dimensions, Materials Research Department, Risø National Laboratory, P. O. Box 49, DK-4000 Roskilde, Denmark

The study of the orientation dependence of elastic strain and crystallographic rotation development during the deformation of polycrystalline materials has been severely hindered by the general inability to non-destructively collect information on individual interior grains during the deformation process. Although theoretical models exist which successfully predict overall properties such as the average texture development and flow stress evolution (e.g. based on Sachs (1928) and Taylor (1938)), there has been to date no method for experimentally verifying the model predictions on the level of an individual grain.

The 3DXRD microscope allows for the measurement of the elastic strain tensor and crystallographic orientation of individual grains imbedded within polycrystalline samples. Furthermore, in-situ studies may be performed using a tensile stress rig. In this way the crystallographic rotation as well as the elastic strain development of individual grains may be experimentally measured for the first time as a function of the applied load.

For both elastic strain and orientation measurements an automated indexing routine (GRAINDEX) is used to group reflections by their grain of origin and fit them to an orientation matrix (Lauridsen *et al.* 2001). In order to measure the elastic strain tensor, the radial shifts of each reflection with respect to zero load conditions are fit using a singular value decomposition routine. Elastic strains can be measured with an error of $5x10^{-5}$ (Margulies *et al.* 2002).

An example of grain rotation measurements are shown in Figure 1. Here the tensile direction of 4 grains are shown in an inverse pole figure at increments of strains from 0 to 11% (Margulies *et al.* 2001). The experimental results are compared to the classical models, and it is found that these models cannot correctly account for the details of individual grain rotations. Further results will be presented which increase the stastistics and allow further conclusions on the current state of texture development modelling.

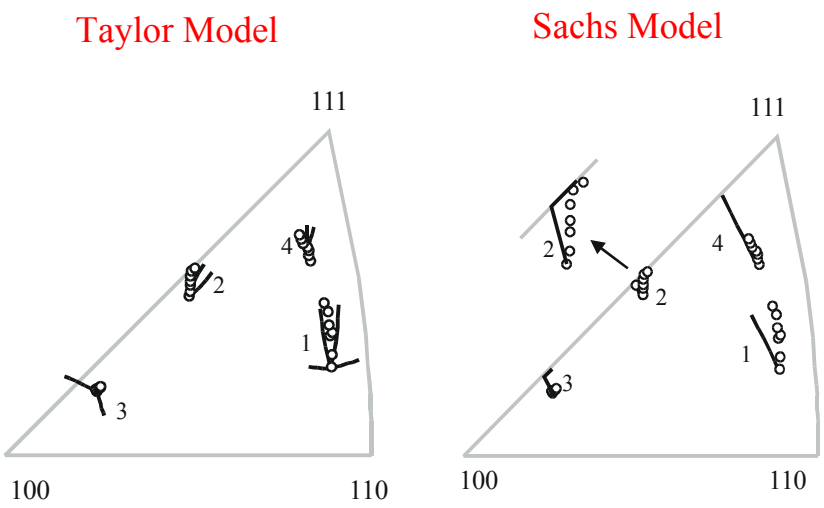

Figure 1. The dynamics of four embedded Al grains during tensile deformation. The open circles represent experimental results at 0, 2, 4, 5, 7, 9, and 11% strain. The lines are the associated predictions based on the Taylor and Sachs models.

Acknowledgements

The authors wish to thank Henning Poulsen, E.M. Lauridsen, R.V. Martins, S.F. Nielsen for experimental assistance, S. Schmidt for assistance in data analysis, G. Winther performed rotation modelling, T. Lorentzen, and T. Leffers assisted in the stress tensor measurements and analysis.

References

Lauridsen, E.M. *et al.* (2001). Tracking: a method for structural characterisation of grains in powders or polycrystals. *J. Appl. Cryst.* 34, 6, 744-750.

Margulies, L., Winther, W., Poulsen, H.F. (2001). In situ measurement of grain rotation during deformation of polycrystals. *Science* 291, 2392-2394.

Margulies, L., Lorentzen, T., Poulsen, H.F., Leffers, T. (2002). Strain tensor development in a single grain in the bulk of a polycrystal under loading. *Acta Materialia* 50, 1771-1779.

Sachs, G. (1928). Zur Ableitung einer Fließbedingung. *Z. Verein Deut. Ing* 72, 734-736.

Taylor, G.I. (1938). Plastic strain in metals. *J. Inst Met.* 62 307-324.

Local strain measurements by using marker particles and synchrotron X-ray absorption tomography

Søren F. Nielsen, Felix Beckmann[1], Casper Thorning, John A. Wert and Henning F. Poulsen

Center for Fundamental Research: Metal Structures in Four Dimensions, Materials Research Department, Risø National Laboratory, P. O. Box 49, DK-4000 Roskilde, Denmark
[1]HASYLAB at DESY, Notkestr. 85, 22607 Hamburg, Germany

Local strains associated with heterogeneous plastic deformation can be measured on the surface of specimens by means of marker grids (e.g. Liu and Fischer 1997). Such local strain measurements can be used to supplement surface measurements of crystal rotation during deformation, by the EBSD method for example (Wert, Huang and Inoko 2001), and the combined results providing four independent parameters describing the local deformation conditions. As there are commonly 12 independent slip systems in metal crystals with cubic lattice symmetry, the combined crystal rotation and grid distortion measurements are still far short of providing enough independently measured quantities to identify the shear amplitude on each slip system. Furthermore, the absence of constraint for surface grains is a severe limitation for comparing the results to models of bulk deformation conditions.

Recent development of a 3D X-ray Diffraction Microscope (Juul Jensen, Kvick, Lauridsen, Lienert, Margulies, Nielsen and Poulsen 2000), developed at Risø and installed in Grenoble, allows for the first time measurement of crystal rotations in bulk samples during deformation. This technique yields three parameters describing the local deformation conditions for grains in a bulk sample. The supplementary information provided by a method for measuring distortions in a bulk sample would increase the number of local parameters to 11, and a combined experiment would allow the shear amplitudes on eight independent slip systems could be deduced within localised regions. This capability would permit testing of competing models describing shear amplitudes on the variously oriented slip systems. The original classical model was proposed more than 70 years ago (Taylor 1938), and various modifications have been developed over the intervening decades (Wert 1998), but a rigorous experimental test of the model predictions has yet to be performed.

In the present research project, we propose to apply the marker grid technique in three dimensions by embedding marker particles in the material prior to deformation and to following the evolution of their position as a function of strain using synchrotron X-ray absorption tomography.

This scheme allows the detection of local scale strain components in three dimensions, precisely the information needed to supplement the bulk crystal rotation measurements.

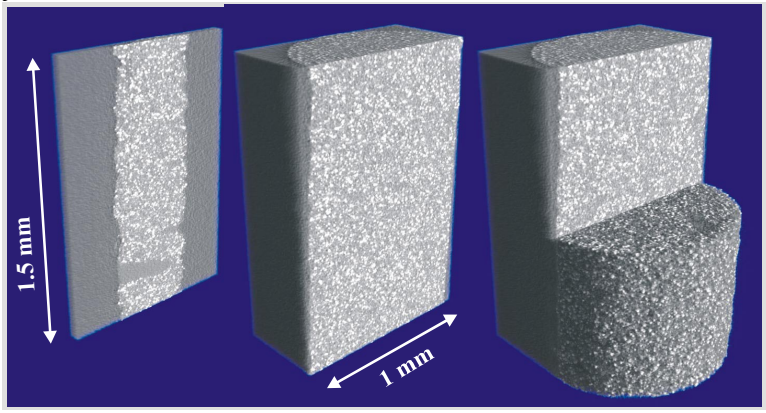

Fig. 1: Visualization of the AlW-sample(about 10% compression). Vertical slices and the 3D representation of the data set are shown. The tomographical scan was performed at beamline BW2 using E=24keV.

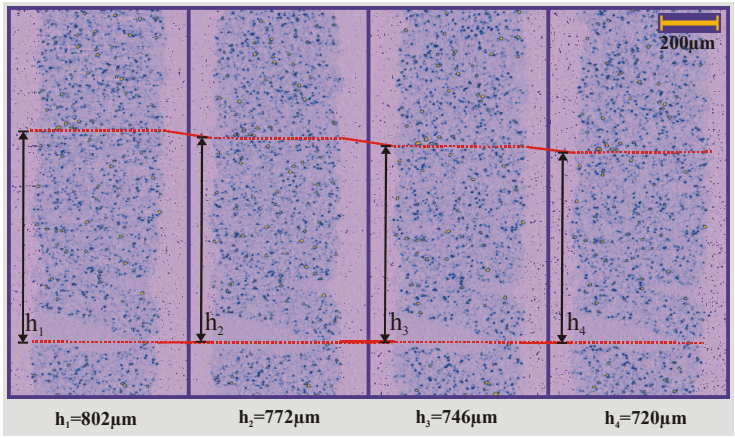

Fig. 2: Vertical Slices through the 3D-reconstruction volumes of 4 tomographical scans of the AlW sample at different deformation steps. Corresponding heights in the different slices draw the compression of the sample. The right slice represents the surface shown on the left side in Fig. 1.

References

Liu Y.L. and Fischer G. (1997) Scripta Mat. 36 1187-1194.

Wert J.A., Huang X., and Inoko F. Deformation bands in a [110] aluminium single crystal strained in tension, submitted to Proceedings of the Royal Society (2001).

Juul Jensen D., Kvick Å., Lauridsen E.M., Lienert U., Margulies L., Nielsen S.F. and Poulsen H.F. (2000). Plastic deformation and recrystallization studied by the 3D x-ray microscope. Mat. Res. Soc. Symp. Proc., 590, 227-240.

Taylor G. I. (1938) J. Inst. of Metals, 62 307-324.

Wert J.A. (1998) Proc. of the Risø Symposium: Modelling of Structure and Mchanics of Materials from Microscale to Product. Editors T. Leffers et al., Risø National Laboratory, 573-584.

Disorientations across deformation-induced boundaries

Wolfgang Pantleon

Center for Fundamental Research: Metal Structures in Four Dimensions, Materials Research Department, Risø National Laboratory, P. O. Box 49, DK-4000 Roskilde, Denmark

During plastic deformation dislocations are accumulated in the crystal and gather into dislocation boundaries. Two different types of dislocation boundaries can be identified (Kuhlmann-Wilsdorf and Hansen 1991): curved and thick cell walls separating individual cells and parallel, straight and extended dense dislocation walls between cell blocks. Boundaries of the first type are expected to originate from stochastically mutual trapping of dislocations (incidental dislocation boundaries, IDBs) whereas boundaries of the second type are a result of differences in the activation of slips systems (geometrically necessary boundaries, GNBs) on both sides. Due to an excess of dislocations of one sign of the Burgers vector, an orientation difference between the two regions next to the boundary arise and increases with strain.

Based on the underlying dislocation dynamics, the evolution of these disorientations is modelled (Pantleon 2002) including statistical trapping of dislocations (Pantleon 1997) and a possible difference in the activated slip systems. The predicted evolution of the mean disorientation angle is in good agreement with experimental data (see Fig. 1). A square root dependence of the disorientation angle on strain is predicted for IDBs, the disorientation angles across GNBs are higher and increase stronger with plastic strain.

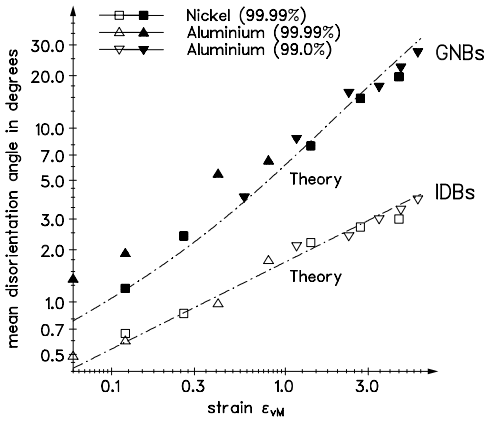

Figure 1: Development of mean disorientation angle with plastic strain for IDBs and GNBs. The theoretically predicted evolution is in good agreement with the experimental data from different materials.

From the model, scaling of the distribution functions can be concluded also, i.e. distributions belonging to different strains coincide after normalization of the disorientation angles by their mean disorientation angle. The shape of the distribution function depends on the number of dislocation sets present in a boundary (Pantleon and Hansen 2002). For a single set a Gaussian distribution, for two sets a Rayleigh distribution and for three sets a Maxwell distribution is predicted. The experimentally observed distributions are best described by a Rayleigh distribution indicating that disorientations are mainly caused by two dislocation sets only.

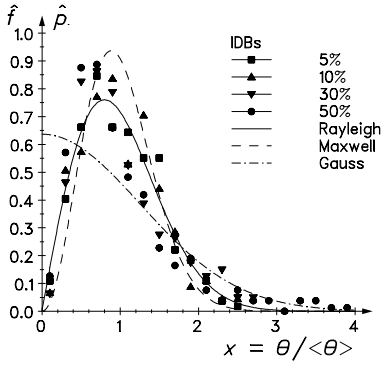

Figure 2: Distributions of normalized disorientation angles. The experimental distributions for cold-rolled aluminium from Hughes et al. (1996) show scaling and are close to a Rayleigh distribution.

Disorientations in neighbouring boundaries are correlated (Pantleon and Stoyan 2001). The average disorientation angle measured over larger distances (across a few boundaries) does not depend on the distance. This is a direct consequence of the limited path of mobile dislocations: dislocations of opposite sign created in the same event can only separate a certain distance. The spatial correlation of disorientations affects the annealing behaviour. During recovery dislocation structures coarsen and the disorientation angle increases towards a saturation value (Pantleon 2002).

References

Hughes D.A., Liu Q., Chrzan D.C. and Hansen N. (1996) Scaling of microstructural parameters: misorientations of deformation induced boundaries. Acta mater. 45, 105-112.

Kuhlmann-Wilsdorf D. and Hansen N. (1991). Geometrically necessary, incidental and subgrain boundaries. Scripta metal. mater. 25, 1557-1562.

Pantleon W. (1997). On the statistical origin of disorientations in dislocation structures. Acta mater. 46, 451-456.

Pantleon W. (2002). Disorientations in Dislocation Structures: Formation and Spatial Correlation. J. Mater. Res. 17, 2433-2441.

Pantleon W. and Hansen N. (2002) Dislocation boundaries - the distribution functions of disorientation angles. Acta mater. 49, 1479-1493.

Pantleon W. and Stoyan D. (2001). Correlations between disorientations in neighbouring dislocation boundaries. Acta mater. 48, 3005-3014, Erratum Acta mater. 48, 4179.

3DXRD – a novel tool for materials science

Henning F. Poulsen

Center for Fundamental Research: Metal Structures in Four Dimensions, Materials Research Department, Risø National Laboratory, P. O. Box 49, DK-4000 Roskilde, Denmark

3D X-Ray Diffraction (3DXRD) microscopy is an emerging tool for fast and non-destructive characterisation of the individual grains inside bulk materials (Poulsen *et al.* 1997, Lauridsen *et al.* 2001, Poulsen *et al.* 2001a). The method is based on diffraction with x-rays from a synchrotron source. With high-energy x-rays (E ≥ 50keV) 3D studies of millimetre - centimetre thick specimens can be performed. Ray tracing with several two-dimensional detectors is applied. This provides a universal method for deriving the position, volume, orientation, elastic and plastic strain for hundreds of grains simultaneously. Likewise for coarse-grained materials grain boundary maps can be generated. With the present set-up at the 3DXRD microscope at ESRF, the spatial resolution is ~ 5 μm, while the orientation resolution is of order 0.1 deg. The main limitation is degree of deformation.

3DXRD microscopy for the first time enables dynamic studies of the individual grains in polycrystals. Note, that conventionally used probes such as electron microscopy are surface probes. These are often not representative with respect to kinetics due to effects such as stress relaxation, pinning and a-typical growth or diffusion.

First, the 3DXRD method will be reviewed with focus on geometric principles and data analysis. (A summary of applications can be found in Poulsen and Juul Jensen 2002). Next, three extensions to the method is outlined:

- *Deformation microstructures*. While the spatial resolution at present prohibits maps of the microstructure, diffracting units (cells, cell-blocks …) of size ≥ 300 nm can be observed, provided they have orientations that are unique within the gauge volume (Poulsen *et al.* 2001b). First results for recovery of a deformed Al single crystal are presented.
- *3DXRD and x-ray tomography.* Algorithms for combined studies are presented (Poulsen and Schmidt 2002). The potential is illustrated with work on wetting of Al by liquid Ga (Nielsen *et al.* 2000), and discussed in relation to fatigue.
- *Materials Engineering*. The 3DXRD method can be modified to provide 3D - or simply depth resolved -texture and stress distributions of interest for engineering. Work is summarised on through-thickness texture gradients in rolled Al (Mishin *et al.* 2000) and

on mapping the residual strain tensor within deformed torsion samples (Martins *et al.* 2001). The spatial resolution in these cases is 50-200 μm.

Acknowledgements

The team presently working with 3DXRD instrumentation and software comprises X. Fu, E.M. Lauridsen, L. Margulies, R.V. Martins, S.F. Nielsen, and S. Schmidt at Risø; A. Goetz and G. Vaughan at ESRF and U. Lienert at APS. Work on wetting was performed with D. Juul Jensen, W. Ludwig (ESRF) and D. Bellet (ENSPG-INPG, St. Martin d'Heres).

References

Lauridsen, E.M. *et al.* (2001). Tracking: a method for structural characterisation of grains in powders or polycrystals. J. Appl. Cryst. 34, 6, 744-750.

R.V. Martins, U. Lienert, L. Margulies, A. Pyzalla (2001). Investigation of the strain distribution in an Al-MMC torsion sample using high energy synchrotron radiation, Proc. of TMS Fall meeting 2001, Indianapolis, Session VI: Affordable Metal-Matrix Composites for High Performance Applications, 285-295.

Mishin, O.V. *et al.* (2000). Application of high-energy synchrotron radiation for texture studies. *J. Appl. Cryst*. 33, 364-371.

Nielsen, S.F., *et al.* (2000). Three dimensional mapping of grain boundaries. Proc. 21st Risø Int. Symp. Mat. Science. Eds: N. Hansen *et al.*, Risø, Denmark, 473-478.

Poulsen, H.F. *et al.* (1997). Applicaton of high-energy synchrotron radiation for structural studies of polycrystalline materials. J. Synchrotron Rad. 4, 147-154.

Poulsen, H.F. *et al.* (2001a). Three-dimensional maps of grain boundaries and the stress state of individual grains in polycrystals and powders. J. Appl. Cryst. 34, 6, 751-756.

Poulsen H.F. *et al.* (2001b). Quantification of minor texture components by hard x-rays. Text. Microstr. 35, 39-54.

Poulsen, H.F. and Juul Jensen, D. (2002). From 2D to 3D microtexture investigations. *Proc. ICOTOM-13,* Seoul, Korea, Mat. Science Forum, 408-412, 49-67.

Poulsen, H.F. and Schmidt, S. (2002). Reconstruction of grain boundaries in polycrystals by filtered back-projection of diffraction spots. J. Appl. Cryst., in print.

Structural Refinement of the individual grains in a polycrystal

Søren Schmidt[1], Gavin B.M. Vaughan[2] and Henning F. Poulsen[1]

[1]Center for Fundamental Research: Metal Structures in Four Dimensions, Materials Research Department, Risø National Laboratory, P. O. Box 49, DK-4000 Roskilde, Denmark
[2]ESRF, BP 220, F-38043 Grenoble Cedex, France.

Today structural refinements are based on either single crystal or powder diffraction data. In many cases neither method is applicable. Specifically, it may be difficult to grow single crystals or the grains need to be studied within their environment. Furthermore, as it is possible to solve and refine much more complex structures from single crystal data than from powder data, it is essentially always of interest to be able to obtain the former sort of data.

We therefore propose to treat the individual grains in the sample (powder, pellet or component) as a collection of single crystals. An indexing and integration program, GRAINDEX, is presented which can sort diffraction spots with respect to grain for hundreds of grains simultaneously (Lauridsen *et al.* 2001). The only limitations are the grain size and the amount of overlap between diffraction spots.

The method is implemented at beamline ID11 at ESRF. Used with hard x-rays (50-100 keV) the extinction and absorption are negligible, while grains of order 300 nm are visible. The method has been initially validated by a study of Al_2O_3 (corundum). An annealed pellet with an average grain size of 20 μm was illuminated with a 50 keV 250 x 250 μm^2 beam. Rotating the sample around one axis with a step-size of 0.1 degree a total of 80.000 spots were detected. Based on an intensity cut 57 of the most intense grains were refined with a typical R_{sym} of <10% after appropriate scaling and filtering. Structural refinements carried out on the thereby obtained integrated peak intensities are essentially identical to that of single crystal data. Studies of more complicated structures are currently underway.

Compared to powder diffraction the method has advantages, in addition to the complexity of the structures which may be treated:

- Instead of average information, distributions are derived.
- Minority phases occupying volume fractions of 10^{-8} or less can be detected.
- Refining individual grains is a natural extension of the 3DXRD concept (Lauridsen *et al.* 2001, Poulsen *et al.* 2001). From 3DXRD the position, volume, crystallographic orientation and strain state of a set of grains are determined simultaneously. Likewise 3D maps of grain boundaries can be derived. Hence,

cross-correlations to other types of structural information can be performed.

References

Lauridsen, E.M., Schmidt, S., Poulsen, H.F., Suter, R.M. (2001). Tracking: a method for structural characterisation of grains in powders or polycrystals. J. Appl. Cryst. 34, 6, 744-750.

Poulsen, H.F., Nielsen, S.F., Lauridsen, E.M., Schmidt, S., Suter, R.M., Lienert, U., Margulies, L., Lorentzen, T., Juul Jensen, D., (2001). Three-dimensional maps of grain boundaries and the stress state of individual grains in polycrystals and powders. J. Appl. Cryst. 34, 751-756.

Experimental observations of local crystal orientation distributions in strained single- and polycrystals.

Casper Thorning, John A. Wert and Xiaoxu Huang

Center for Fundamental Research: Metal Structures in Four Dimensions, Materials Research Department, Risø National Laboratory, P. O. Box 49, DK-4000 Roskilde, Denmark

A series of experiments (Wert, Huang and Inoko, 2002) have been conducted as follows to examine the distributions of local crystal orientations in single crystals and polycrystals resulting from straining by rolling or tension:

1. An Al single crystal was strained 30% in tension. The crystal was initially oriented with [110] parallel to the tensile axis and $(1\,\bar{1}\,1)$ parallel to the front face. After deformation, crystal orientations were measured by means of the EBSD technique over a large area across the front face of the specimen and on a through-thickness area of the cross section, revealing local crystal rotations associated with the deformation bands that formed during straining.

Mapping the crystal rotations as the rotation axis/angle pairs reveals evident misorientation heterogeneities corresponding to the deformation bands. Contrary to the predictions of standard analysis, distinct domains of the banded structure showed rotation about the tensile axis, whereas rotation about the front face normal dominated in other areas. An analysis was made to connect the local crystal orientation measurement to local slip patterns, under the assumption that slip was restricted to the four critically stressed slip systems in the above mentioned load situation, namely the a1, -a2, b1, and -b2. Duplex slip on a coplanar combination of the four critically stressed slip systems results in a rotation of the tensile axis and a rotation about the tensile axis that distorts the original rectangular cross section geometry. Mechanical constraint of the tensile axis produces crystal rotation about axes normal to it. Similarly, the constraint on the front and back faces of the crystal imposed by the grips introduces a rotation of the crystal about the tensile axis.

2. EBSD measurements were made along a line parallel to the normal direction (ND) in 50 % rolled Al single crystals initially having Goss, Cube, and Rotated Cube orientations respectively (Wert 2002). The measurements reveal typical + - + - macroscopic crystal rotation patterns, with rotation primarily about the transverse specimen axis (TD) and with a rotation amplitude depending on the initial orientation. A macroscopic + - + - pattern of shear in the rolling plane in the rolling direction known as redundant shear is known to develop along the ND as a consequence

of the geometry of material flow through a converging channel, as is the case in rolling. The presence of such a shear pattern in the rolled single crystals was demonstrated in a qualitative way by the means of marker wires.

The imposed displacement gradient components can be accommodated by any two coplanar slip system pair, or by an equivalent slip system pair accommodating the displacement gradient components of the physical slip systems. When the two equivalent slip planes make equal angles to the rolling plane, a non-zero e_{13} component results in unequal shear amplitudes on the two equivalent planes, which in combination with the constraints on the upper and lower specimen boundaries induces crystal rotation about the line of intersection of the two equivalent systems, i.e. the TD axis. It follows that when the angle between the equivalent slip planes and the rolling plane is small the slip process is more closely aligned with the imposed shear deformation and only a modest imbalance in shear amplitudes on the two equivalent slip systems is required to accommodate e_{13} (Wert and Huang 2002). The rotation amplitude about the TD axis is consequently modest, whereas the opposite is the case for large angles between equivalent slip planes and rolling plane.

3. A polycrystalline Cu specimen with a grain size of ~ 250 microns was strained 10 % in tension.

EBSD maps with a resolution of 2 microns were made on individual grains of known orientation prior to and after straining. Mapping the local crystal misorientations of the strained crystal to the unstrained crystal revealed evident crystal rotation heterogeneities across the grain. In particular, larger rotations are seen in areas adjacent to some neighbouring grains than in areas adjacent to others. Likewise, areas adjacent to twins are seen to exhibit large rotations. Less crystal rotation is seen in the centre of the grain.

It can be concluded from the first two studies that crystal rotation heterogeneities and patterns of such develop in crystals during deformation as a result of mechanical constraints imposed on the crystal. Therefore it seems likely that the development of heterogeneities in individual grains in polycrystals should be at least in part governed by the mechanical constraints imposed on them by the grains surrounding them.

References:

Wert J.A., Huang X. and Inoko F. (2002). Deformation Bands in a [110] Aluminium Single Crystal Strained in Tension, Proc. Roy. Soc., Article in Press.

Wert J.A. (2002). Macroscopic crystal rotation patterns in rolled aluminium single crystals, Acta Mater., 2002, Article in Press.

Wert J.A. and Huang X. (2002): Extended planar boundary inclinations in fcc single crystals and polycrystals subjected to plane strain deformation, Submitted to Phil. Mag.

Preferred planes of deformation induced dislocation boundaries

Grethe Winther

Center for Fundamental Research: Metal Structures in Four Dimensions, Materials Research Department, Risø National Laboratory, P. O. Box 49, DK-4000 Roskilde, Denmark

Literature contains apparently conflicting results on the planes of deformation induced dislocation boundaries. Some studies report that certain macroscopic planes are preferred boundary planes. Other studies have found that boundaries preferentially align with specific planes in the crystallographic lattice.

Preferred macroscopic boundary planes

In plane strain compression, which is the ideal deformation mode usually assumed for homogeneous rolling, there are two perpendicular macroscopically most stressed planes. These are inclined ±45° to the rolling direction in the longitudinal plane. Boundaries in metals deformed to moderate strains ($\varepsilon<1$) are predominately found in the vicinity of these two planes (Bay, Hansen and Kuhlmann-Wilsdorf 1989) but the mean trace angle in the longitudinal sample plane varies somewhat around 45°. Also the spread of boundary planes around these planes is typically more than 20°.

In tension the macroscopically most stressed planes are tangents to a cone inclined 45° to the tensile axis and the number of most stressed planes is infinite. Experimental data have been found to agree well with boundaries lying close to this cone (Zhu and Sellars 2001).

Preferred crystallographic boundary planes

In many studies the boundary plane has been related to the slip planes. Especially for single crystals boundaries have been reported to align with slip planes (Basinski and Basinski 1964). Many of these studies have established that the boundaries are not exactly on slip planes but deviate a few degrees from these. There are, however, also many observations of boundaries lying far from slip planes in both single (Kawasaki and Takeuchi 1980) and polycrystals (Bay et al. 1989).

It has recently been found for both rolling and tension that there is a strong correlation between the orientation of the boundaries and the orientation of a grain so that some grain orientations have boundaries close to slip planes and other orientations have boundaries lying far from slip planes (Liu and Hansen 1995).

In a detailed investigation of the crystallographic orientation of dislocation boundaries as a function of grain orientation for a tensile deformed aluminium polycrystal (Winther, Huang and Hansen 2000) it was found that the crystallographic planes on which extended planar dislocation boundaries lie have very well-defined geometric relations to the slip planes. This is also the case when the boundaries lie far from the slip planes.

Comparison of macroscopic and crystallographic preferences

Boundaries do not always deviate from the slip plane to get nearer to the macroscopically most stressed plane but may also get further away from this plane. Macroscopically most stressed planes (in analogy with slip planes) are therefore not *per se* preferred boundary planes.

Furthermore, only a few different boundary planes are observed in a grain/crystal even though the number of macroscopically most stressed planes is infinite in tension due to the rotational symmetry. The planes of the observed boundaries are fixed in the crystallographic lattice where there is no rotational symmetry around the tensile axis. These findings indicate that crystallography is a more important factor controlling boundary plane orientation than macroscopically most stressed planes.

The conclusion is that boundaries have both macroscopic and crystallographic preferred orientations but that the macroscopic preference is weaker than the crystallographic:

- In the macroscopic sample co-ordinate system boundaries cluster around the most stressed planes. However there is a significant spread around these macroscopic planes and no clear geometric relation between these planes and boundary planes.
- In the crystallographic lattice there is an unambiguous geometric relationship between boundary planes and slip planes. The deviation of a boundary plane from the nearest slip plane varies systematically with the grain orientation.

References

Basinski, Z. S. and S. J. Basinski (1964). Dislocation distributions in deformed copper single crystals. Philosophical magazine 9, 51-80.

Bay, B., N. Hansen and D. Kuhlmann-Wilsdorf (1989). Deformation structures in lightly rolled pure aluminium. Materials science and engineering A113, 385-397.

Kawasaki, Y. and T. Takeuchi (1980). Cell structures in copper single crystals deformed in the 001 and 111 axes. Scripta Metallurgica 14, 183-188.

Liu, Q. and N. Hansen (1995). Deformation microstructure and orientation of FCC crystals. Phys. stat. sol. (a) 149, 187-199.

Winther, G., X. Huang and N. Hansen (2000). Crystallographic and macroscopic orientation of planar dislocation boundaries - correlation with grain orientation Acta Mat. 48, 2187-2198.

Zhu, Q. and C. M. Sellars (2001). Evolution of microbands in high purity aluminium-3%magnesium during hot deformation testing in tension-compression. Scripta Mat. 45, 41-48.

Experimental observation and modelling of average lattice rotations of individual grains in columnar grained nickel

Guilin L. Wu[1], Grethe Winther[2], Qing Liu[1]

[1]Department of Materials Science and Technology, Tsinghua University, Beijing, 100084, China
[2]Center for Fundamental Research: Metal Structures in Four Dimensions, Materials Research Department, Risø National Laboratory, P. O. Box 49, DK-4000 Roskilde, Denmark

Experimental verification of polycrystal plasticity models for prediction of deformation textures has so far only been possible at the bulk level, i.e. by averaging over all grains, because of lack of grain-scale experimental data. Recently, lattice rotations of individual grains deeply embedded in a polycrystal has been measured *in-situ* by 3-dimensional X-ray diffraction (3DXRD) (Margulies, Winther and Poulsen 2001). Access to this technique is however limited. Use of columnar grained samples has been suggested as a complementary technique (Wu, Godfrey and Liu 2002).

Columnar grained Ni with a strong <001> fibre texture was produced by directional solidification. The material has a coarse grain structure with average grain diameter of 600μm in the rolling plane and ranging from the top to the bottom of the material. Samples of size 10×30×2-4 mm^3 were rolled to reductions of 10%, 30% and 50% at ambient temperature under homogeneous deformation conditions. After each deformation step, a layer of about one quarter thickness of the sample was removed from the rolling surface.

Orientation changes in the rolling plane for a number of individual grains were measured by the electron back-scatter pattern (EBSP) technique. Grains initially lying within 5° of three different initial orientations, cube orientation and cube orientations rotated 22.5° and 45° around ND, were investigated in detail. From the average orientation evolution of each grain, it was found that grains with close initial orientations almost rotate in same manner.

The FC Taylor model was applied to predict the rotation of each grain. At the bulk scale, the predicted and measured textures are comparable. In spite of the success at the bulk scale, however, the Taylor model predictions for individual grains are not perfect. For grains initially close to the cube orientation the model predicts the rotation direction well but the magnitude of the rotation is significantly smaller than experimental. 67%

of the predicted rotation paths for the 12 grains initially close to the 45° ND rotated cube orientation match the experimental ones well. Finally, only the rotation of 25% of the 12 grains initially close to the 22.5° ND rotated cube is well predicted. Figure 1 below gives two examples of the results.

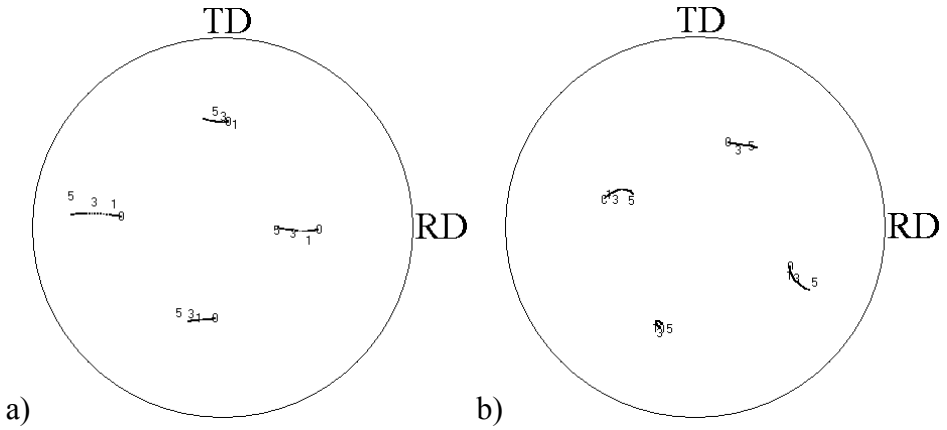

Figure 1: Pole figures of experimental results and modelled results of two grains initially close to a) 45° ND rotated cube and b) 22.5° ND rotated cube. In each pole figure, 0, 1, 3 and 5 represent the average orientation of the grain rolled to 0%, 10%, 30% and 50% reduction, respectively. The line represents the predicted rotation paths.

Acknowledgements

The authors wish to thank Drs. N. Hansen and D. Juul Jensen for their thoughtful comments and discussions. Part of the work is supportted by National Nature Science Foundation of China under contract number of 59825110.

References

Margulies L., Winther G. and Poulsen. H. F. (2001). In situ measurement of grain rotation during deformation of polycrystals. Science, 291 (23), 2392-2394.

Wu G.L., Godfrey A., Liu Q. (2002). Texture and deformation structure evolution during rolling of individual grains of columnar grain nickel. ICOTOM 13, South Korea, In Press.

SEM-ECC investigation of microstructural evolution during cyclic deformation of ultrafine grained copper processed by ECAP

S. D. Wu, Z. G. Wang, C. B. Jiang and G. Y. Li

Shenyang National Laboratory for Materials Science, Institute of Metal Research, Chinese Academy of Sciences, Shenyang 110016, P.R. China

Ultrafine grained (UFG) materials processed by equal channel angular pressing (ECAP) have attracted much of attention of many researchers during past decade due to their interesting physical and mechanical properties. Studies of the cyclic deformation and fatigue properties of UFG materials have been mainly focused on copper because copper serves as a model material for academic research. It is commonly accepted that UFG copper will suffer severe cyclic softening and a deterioration of the fatigue life in constant plastic strain-controlled testing compared with its coarse grain counterpart. Shear banding and grain coarsening are considered to be the major factors responsible for cyclic softening and a shorter fatigue life in term of low cyclic fatigue, whereas up to now their formation mechanisms are still open questions.

The objectives of the current study are twofold. One is to verify the hypothesis that there is a relationship between shear banding and grain coarsening by examining the microstructure in the vicinity of shear bands and find out some clues to the formation of shear bands. The other is to investigate the evolution of grain coarsening in the course of cyclic deformation.

Electron channeling contrast in scanning electron microscope (SEM-ECC) was used in the present study because it can disclose the microstructure in any special sites within the gauge part of specimen and trace the development of some interesting microstructural features during cyclic deformation. SEM-ECC inspections of microstructure in the vicinity of shear bands were performed on the cyclically deformed UFG copper (99.98 % purity) specimens. Figure 1 shows a typical example of shear bands together with nearby microstructures. It can be seen that no significant grain coarsening occurred in the vicinity of shear bands. Therefore, it is concluded that there is no relationship between shear bands and grain coarsening. The formation of shear bands is discussed on the basis of oriented distributions of defects along the shear plane of last pressing and reversible cyclic deformation.

A series of SEM-ECC observations were conducted on the high purity UFG copper (99.999% purity) specimen cyclically deformed at a plastic

strain amplitude of 5×10^{-4}. The testing was interrupted at 1500, 2500 and 4500 cycles to investigate grain coarsening in the course of cyclic deformation. As shown in figure 2, an additional 3000 cycles caused plastic deformation to take place mainly within the less coarsened grain within the dashed square, resulting in the formation of dense slip bands and a fully developed dislocation wall structure as well as an increase in the grain size. Figure 2c shows this grain under higher magnification. A model is proposed to account for the evolution of grain coarsening, emphasizing the role of interaction between the cyclic deformation and the growth of coarsening region.

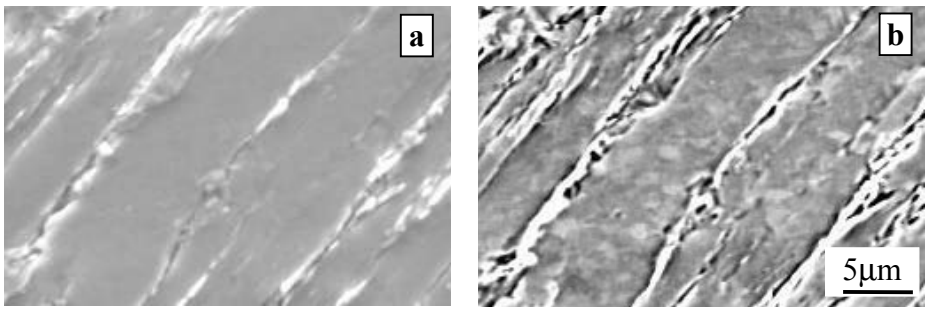

Figure 1. SEM (a) and SEM-ECC (b) images of shear bands along with microstructures nearby.

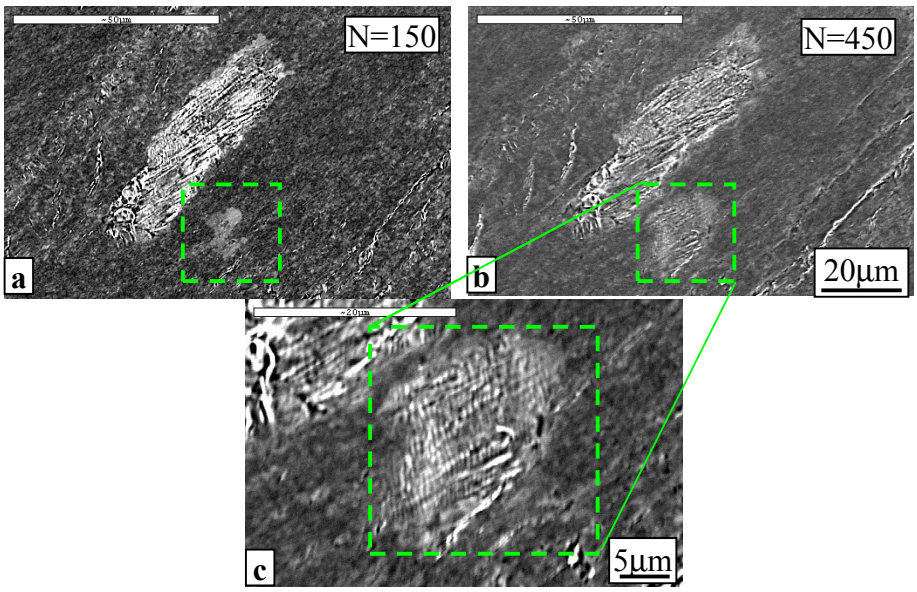

Figure 2. SEM-ECC images of a band-like coarsening region with a less coarsened grain of irregular shape nearby in a specimen cyclically deformed at constant plastic strain amplitude of 8×10^{-4} for (a) 1500 cycles and (b) 4500 cycles. (c) shows the less coarsened grain within the dashed square (b) under higher magnification.

TEM characterization of surface and interface structures

Qingfeng Xing

Center for Fundamental Research: Metal Structures in Four Dimensions, Materials Research Department, Risø National Laboratory, P. O. Box 49, DK-4000 Roskilde, Denmark

Transmission electron microscopy (TEM) is a powerful tool in the investigation of material surfaces and interfaces because it can extract both structural and compositional information from a region of about micrometer to a resolution on the atomic scale (Williams and Carter 1996, Spence and Zuo 1992). Surface and interface problems usually involve sampling a surface or interface region and the sample width depends on how much the region differs from the bulk material. The width usually covers a region from the micrometer level to the atomic level. Surface and interface characterizations can be summarized as: (i) morphology or image observation such as a whole picture of the microstructure; (ii) dislocation measurement; (iii) crystallography such as crystallographic orientation and symmetry determination; (iv) phase identification; (v) chemical analysis; and (vi) elastic stress measurement.

Specimen preparation is state-of-the-art and fundamental to TEM examination. TEM foils include planar view and cross-sectional view of a surface or interface. Only specimen preparation methods for the cross-sectional view of a surface or a macro interface are reviewed here because they are the most difficult to prepare. If a cross-sectional view of a surface region is wanted, it is a good idea to adhere two surfaces together with an epoxy resin in starting the specimen preparation. This method has two advantages: enhancing the thin area of the region of interest and protecting the surface from contamination and damage during following steps. When the bulk specimen is thin, support materials should be adhered on both sides. For soft or brittle material, a cross-sectional foil should be strengthened by a copper or molybdenum mesh on one side to prevent plastic deformation or fracture during the handling process. When a metal/ceramic or ceramic/ceramic interface is involved, ion milling and focused-ion beam (FIB) milling methods are the chosen methods for final thinning. The ion-milling techniques are complicated and the following points are important: selecting between one beam and two beams during ion milling, controlling the rocking angle of the specimen or shielding the beam or beams from bombing the specimen along the interface, selecting suitable parameters of the glance angle, the accelerating voltage and the current of the ion beam or beams. A lower glance angle, and lower accelerating voltage and current can reduce the preferential milling of one material, but the thinning speed will be reduced. Usu-

ally, the parameters of large values are chosen in the beginning and changed to smaller values after a period of time. If a metal surface or an interface between identical metals is investigated, electro-jetting method is the best final thinning way because no damage is introduced during jetting. To get a thin area including the surface or interface, it is suggested to paint a glue on the foil and leave the surface or interface and its nearby region uncovered. If an oxide film on the foil surfaces is a problem, an ion-milling machine can be used to remove the oxide film.

Many TEM techniques are applied such as bright-field, dark-field, and weak-beam methods; selected-area electron diffraction (SAD), convergent-beam electron diffraction (CBED) or micro-beam diffraction (MBD), high-resolution electron microscopy (HREM), energy dispersive X-ray spectroscopy (EDX), and electron energy-loss spectroscopy (EELS). Difficulties arise in TEM examinations if a region is smaller than tens of nanometres. In this case, a field-emission electron, a charge-coupled device (CCD) detector or image plate (IP) system, and an energy filter are essential.

An example is given in the Figure, which shows an Al/glass interface achieved by anodic bonding.

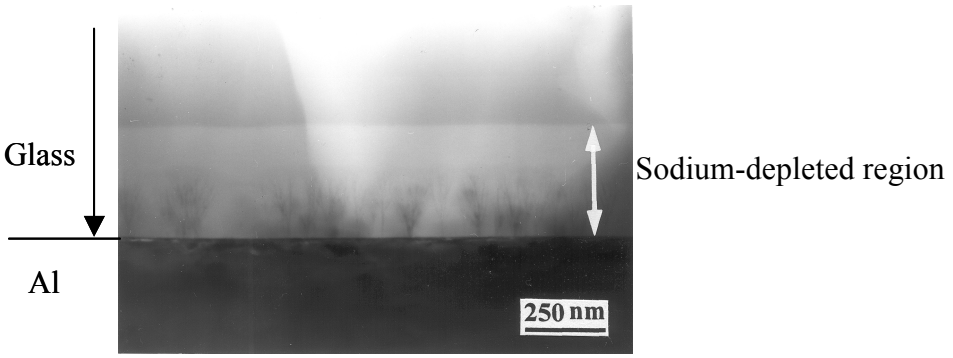

Figure: Interface of Al/glass bonded at 623 K, 500 V and 11.4 ks. The cross-sectional foil was prepared by ion milling. The γ-Al_2O_3 trees grew from the aluminium into a sodium-depleted region of glass.

Acknowledgements

The author thanks Drs Xiaoxu Hang and Niels Hansen for helpful discussions and suggestions.

References

Williams, D. A., and Carter, C. B., 1996, Transmission Electron Microscopy, Plenum Press, New York.

Spence, J. C., and Zuo, J. M., 1992, Electron Microdiffraction, Plenum Press, New York and London.

Characterization of deformation behavior and texture formation in a magnesium alloy AZ31 with initial texture

Ping Yang[1] and G Gottstein[2]

[1]School of Materials Science and Engineering, University of Science & Technology, Beijing 10083, P.R. China
[2]Institut für Metallkunde und Metallphysik, RWTH Aachen, 52056, Aachen, Germany

Magnesium is the lightest metallic structural material with high specific strength and therefore is widely used in automotive, electronics and aerospace industries. However, its plastic formability is rather low at room temperature due to its insufficient basal slip system of hexagonal structure. To improve its formability different methods are chosen, for instance, to refine grain size, to activate new slip systems of prism and pyramid slips or dynamic recrystallization, or even super plasticity by increasing deformation temperature, or to introduce plastic secondary phase as in Mg-Li alloy. This paper aims to explore the possibility of improving plasticity of magnesium alloy by utilizing its anisotropy based on three early results. Early investigation revealed that initial textures of polycrystalline magnesium obtained from hot rolled plate affected strongly deformation behaviors and the texture evolution was followed at 100~200°C. The best plasticity was found in the sample with the initial texture of $\{10\ \bar{1}0\}$ $<11\ \bar{2}0>$. Deformation accommodation of grains was greatly improved during deformation at 200°C and grains became elongated. It revealed the potential of improving the plasticity of magnesium alloy by adjusting initial textures. As a further work this paper investigated the deformation behaviors and texture formation in magnesium alloys AZ31 with initial textures.

Materials used were a hot extruded bar with pronounced fiber textures of $<1\ \bar{1}00>$and $<11\ \bar{2}0>$ ||extrusion axis and a hot rolled plate with strong <0001>||ND of magnesium alloy AZ31. To eliminate deformed grains samples were annealed at 420°C for 6 hours for extruded bar and 500°C for 2h for hot rolled plate. The grain size of hot-rolled plate was fine (about 25μm) and homogeneous, while that in extruded bar was 34μm and inhomogeneous with some grains being large than 400μm. Different types of samples were sectioned from annealed samples. Channel die compression was carried out to realize plane-strain compression at different temperatures. The samples were polished in an AC-2 electrolytic solution and were etched in a solution of picric and acetic acid. Six

pole figures of (10 $\bar{1}$0), (0002), (1 $\bar{1}$01), (1 $\bar{1}$02), (11 $\bar{2}$0) and (1 $\bar{1}$03) were measured to calculate orientation distribution function (ODF). EBSD analysis was performed in an SEM LEO-1450 equipped with HKL Channel 4 system.

It was found that there was a relationship between deformation mechanisms and initial textures at low temperatures. The prism texture (0,60,0) in sample XZ was rather stable, but the component (0,70,30) was unstable manifesting the operation of double prism slips. The weak components (90,25,0) and (75,20,30) were resulted by {10 $\bar{1}$2} twinning. The scattering of (0,90,0) around RD can not be explained only with prism slip, rather it should also be related with basal slip or even pyramid slip {10-11}<1-210>. The rotation caused by double prism slips is opposite to that by double basal slips. Therefore there is a balance between them leading to the scattering around RD. In sample ZY a strain of 25% at 97°C rotated almost all grains to basal texture orientation (ϕ1,0,0) and (ϕ1,0,30) i.e., <0001>||ND. This is due to the {10-12} twinning of c-axis tension, which was favored when c-axes of grains were parallel to RD. This indicates that initial orientations were very unstable. EBSD analysis verified that the twin is {10-12} type with an orientation relationship of 86.3<11-20>. The scattering of basal orientation around TD in sample XY favored the operation of basal slip. The enhancement of (30,0,0), i.e., {0001}<2 $\bar{1}$ $\bar{1}$0> component, can be ascribed to the single basal slip, because double basal slip will generate (0,0,0) orientation, i.e., {0001}<10 $\bar{1}$0>. According to trace analysis in microstructure it is known that in addition to basal slip the {10 $\bar{1}$1} twinning of C-axis compression also occurred in basal oriented grains, however, referring to texture it is evident that only basal slip contributed to texture formation.

It was also found that initial textures influenced dynamic recrystallization. The bulging mode and subgrain rotation were detected to be the nucleation mechanisms of dynamic recrystallization. Dynamic recrystallization was slower in samples with less inhomogeneities (shear bands). During dynamic recrystallization there were texture changes in samples XZ and ZY, but not in XY. Furthermore the texture became weaker in sample ZY and stronger in sample XY. However, new grains evolved into basal orientation in different speeds as strain increased. In sample ZY grains rotated through different orientation paths at two temperatures. Whereas grains twined before recrystallization at 266°C, twinning did not operate in large scale at 340°C leading to a nearly random texture.

EBSD analysis revealed that new grains were scattered from neighboring deformed matrix. As strain increased new grains rotated gradually to basal orientation. Besides the orientation relationships of ~30°<0001> and ~90°<11 $\bar{2}$0> often existed in textured samples. This is typical in magnesium of hexagonal structure. The former corresponds to the maximum misorientation in grains with approximate orientation and the latter corresponds to the twinning relationship.

Interfacial energy of B1-precipitates with iron

Z.-G. Yang[1] and M. Enomoto[2]

[1]Department of Materials Science and Engineering, Tsinghua University, Beijing 100084, P. R. China
[2]Department of Materials Science, Ibaraki University, Hitachi 316-8511, Japan

The interfacial energy of non-metallic inclusions with iron may play an important role for microstructure control in steel and steel welds, e.g. the fabrication of fine, interweaving ferrite microstructure. A discrete lattice plane, nearest neighbour broken bond (DLP/NNBB) model was employed to study the chemical interfacial energy of B1(NaCl)-type inclusions in austenite and ferrite (Yang and Enomoto 1999, 2001, 2002). In this work, the anisotropy of interfacial energy and the corresponding equilibrium shape of B1-precipitates with liquid iron are studied by the NNBB model. The chemical interfacial energy, σ, is calculated as the difference in free energy between the interfacial region and the bulk. Under the assumption that the entropy term is insignificantly small, the interfacial energy is given by,

$$\sigma = E_{\xi/L} - \frac{E_{\xi/\xi} + E_{L/L}}{2} \qquad (1)$$

where $E_{\xi/L}$ and $E_{\xi/\xi}$ are the sum of the bond energy across the liq.Fe/compound interface and across the plane of the same orientation in the compound phase, respectively. $E_{\xi/L}$ is calculated from,

$$E_{\xi/L} = n_s Z e_{FeM} + n_s' Z' e_{FeI} \qquad (2)$$

where $Z=\Sigma\, jz_j$, $Z'=\Sigma\, j'z_j'$, n_s and n_s' are the number of metal (M) and non-metallic (I) atoms per unit area of the interface, respectively, and z_j and z_j' are the coordination number of the nearest neighbour M and I atoms to an M atom (the liquid phase is regarded as pure Fe). $E_{L/L}$ is the sum of the bond energy across the plane in the liquid (approximately two times of the liquid surface energy). In an earlier model (Skapski 1956) it was considered that the structure of the liquid is unaltered up to the interfacial plane. Later, it was considered that the liquid phase is adjusted to some extent to the crystal interface in the immediately adjacent layers. On the basis of the hard sphere model it was proposed that the number of atoms in the 1st layer is approximately 0.75 of that in the crystal plane (Spaepen 1975). However, it is only for a close-packed crystal plane and the knowledge on the structure of high index interfacial planes is lacking. Under these circumstances it is assumed that $E_{\xi/L}$ is independent of the interface orientation, which implies that the anisotropy of the interfacial energy comes only from the orientation dependence of $E_{\xi/\xi}$. An alterna-

tive is to assume that the atom arrangement in the layers of the liquid adjacent to the interface has an almost coherent structure with the crystal phase within the 1st neighbour distance. In this case both $E_{\xi/L}$ and $E_{\xi/\xi}$ are the same as the fcc Fe/compound interfaces and only $E_{L/L}$ is independent of the orientation. The calculation is conducted with the e_{FeM} and e_{FeI} values for TiN (Yang and Enomoto 2001). Figure 1a is the (110) section through the polar plot of the chemical part of fcc Fe/TiN interfacial energy and Fig.1b is the three-dimensional polar plot and the equilibrium shape derived from Wulff construction. In contrast to a binary fcc/fcc interface {100}-type interfaces have the minimum energy and {111}-type interfaces have the maximum energy. This is because the contribution from strong M-I interaction is greater than the contribution from M-M interaction. The corresponding equilibrium shape is a cube (Yang and Enomoto 2001). Figure 2a is the (110) section through the polar plot of TiN/liq.Fe interfacial energy calculated assuming a constant $E_{\xi/L}$ value, the value of which was chosen such that {100}-type interfaces has a similar energy to that in Fig.1. Although the anisotropy is considerably different from the TiN/fcc Fe interfaces, the equilibrium shape is likely to be a cube, due to the deep cusp at {100} orientation (Fig.2b). This agrees well with some experimental results.

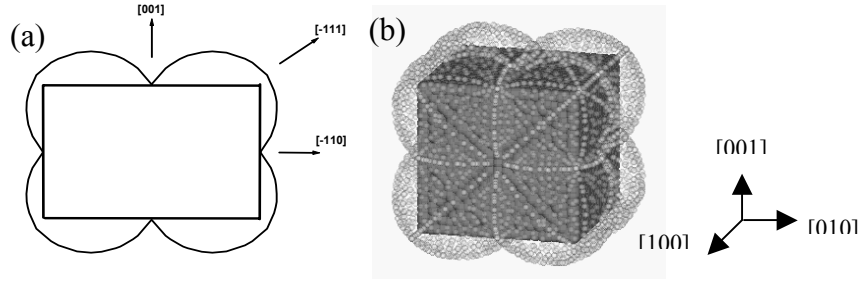

Figure 1: (a) {110}-section of the polar plot of the chemical interfacial energy and (b) the corresponding Wulff construction for the equilibrium shape of TiN in fcc Fe.

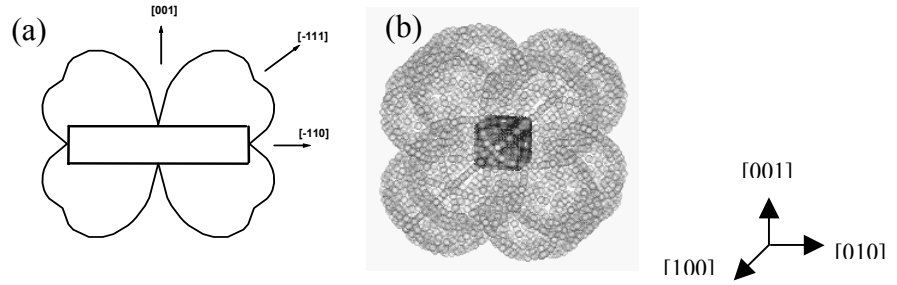

Figure 2: (a) {110}-section of the polar plot of the chemical interfacial energy and (b) the corresponding Wulff construction for the equilibrium shape of TiN in liq.Fe.

References

Skapski A.S. (1956), Acta Met. 4, 576
Spaepen F. (1975), Acta Metall. 23, 729
Yang Z.-G. and Enomoto M. (1999), Acta mater. 47, 4515
Yang Z.-G. and Enomoto M. (2001), Metall. Mater. Trans. A, 32A, 267
Yang Z.-G. and Enomoto M. (2002), Mater. Sci. Eng. A 332, 192

Formation of nanostructured surface layer on AISI 304 stainless steel by means of surface mechanical attrition

H.W. Zhang[1.2], Z.K. Hei[2], L.H. Qian[1], G. Liu[1], J. Lu[3] and K. Lu[1]

[1]Shenyang National Laboratory for Materials Science, Institute of Metal Research, Chinese Academy of Sciences, Shenyang 110016, P.R. China
[2]Institute of Materials & Technology, Dalian Maritime University, Dalian 116026, P.R. China
[3]LASMIS, University of Technology of Troyes, 10000, Troyes, France

Surface mechanical attrition (SMA) is a newly-developed technique that can produce nanostructured surface layers (i.e. surface nanocrystallization - SNC) in various materials. The grain refinement mechanism for iron and Al-alloys, with medium-high stacking fault energy (SFE), is believed to be related to dislocation behavior. Since the SFE is one of the key factors determining the deformation manner, it is necessary also to examine the SNC behavior as well as the grain refinement mechanism for materials with low SFE values under SMA treatment. To date, there is a lack of knowledge of this aspect. AISI 304 stainless steel is a widely-used engineering material with very low SFE value (16.8 mJ/m^2), so the objective of present investigation is to study the SNC of AISI 304 stainless steel. The experimental results show clearly that a nanostructured surface layer is formed during SMA treatment. Based on the detailed cross-sectional TEM and SEM observations, a grain refinement mechanism, occurring in several stages, for 304 stainless steel under SMA treatment is proposed.

Formation of planar dislocation arrays and twins. Strain-induced dislocations in the present austenite phase (f.c.c.) slip mainly on their respective {111} planes, forming regular dislocation grids. Mechanical twins are the decisive features of the AISI 304 stainless steel during the course of SMA treatment. Owing to the increasing of strain and strain rate at smaller depths, the density of twinning increases. Formation of mechanical twins introduces large-angle boundaries (Σ3 etc.) to subdivide the deformed grains.

Grain subdivision and martensite transformation. When two sets of mechanical twins are activated to accommodate the deformation, twin-twin intersections will be inevitable, to produce rhombic blocks, and other shaped blocks with different sets of twins intersections. Twin-twin intersections produce rhombic blocks with changed orientations and bordered by large-angle boundaries (Σ3 and Σ9 etc). Additionally, strain-induced martensite phases are formed at intersections of twins where strains are large enough to induce the martensite transformation. With a

decrease of depth from the top surface, both strain and strain rate increase, so that the martensite transformation is enhanced. Apparently, twin-twin intersections not only subdivide the original grains efficiently through introducing different boundaries (Σ3, Σ9, and other boundaries), but also induce a martensite transformation (introducing phase boundaries) leading to formation of refined microstructures.

Nanocrystallite formation. In the top treated surface layer of the AISI 304 stainless steel, nanometer-sized martensite grains with random orientations are formed. Formation of the nanocrystallites may be attributed to three distinct effects in the top layer: (i) a very large strain; (ii) an extremely large strain rate (estimated to be about 10^3~10^4 s^{-1}); and (iii) multidirectional repetitive loading by shots. The remarkably increased strain and strain rate may activate a high density of multi-system mechanical twins to accommodate the straining. The thickness of the twins will be much reduced with the extremely high strain and strain rate, feasibly in the nanometer regime. These ultrafine twin-twin intersections may result in grain subdivision as well as a martensite transformation in the nanometer scale. The multidirectional repetitive loading may also facilitate formation of different twin systems, leading to mechanical twins intersecting not only with the current co-operative twin systems, but also with the previously generated mechanical twins. Obviously, these three effects in the top surface layer contribute cooperatively to refinement of the original grains into the nanometer regime. Figure 1 illustrates schematically the overall sequence of microstructural evolution.

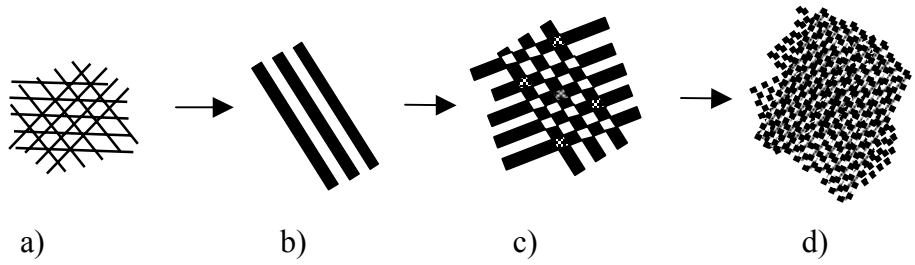

Figure 1. Schematic illustration of microsturctural evolution and grain refinement process in the surface layer during the SMA treatment of the AISI 304 stainless steel; (a) formation of planar dislocation arrays in different slip plane, (b) formation of twining, (c) intersections of twins givnes grain subdivision and martensite transformations, (d) formation of refined grains with random orientations.

Investigation of medium temperature phase transformations in AA1235 aluminium sheets for foil

Jing Zhang and Fusheng Pan

College of Materials Science & Engineering, Chongqing University, Chongqing 400044 , P.R. China

To obtain thin high quality aluminium foil, it is important to use high quality aluminium sheet with reasonable internal structure to decrease the deformation resistance and the work-hardening rate so as to increase the rolling performance (Matsui 1990). Before cold rolling to the final foil product, aluminium sheet generally undergoes an interstage "recrystallisation annealing" treatment. The interstage annealing however promotes more than just recrystallisation, and has a great effect on rolling performance of aluminium sheets and final qualified rate of foils, though only few studies have been made on the microstructural effects of the interstage annealing (Shoji and Fukijura 1990). A systematic study has therefore been carried out on the formation and transformation of intermetallic compounds in AA1235 aluminium sheets for foils in the medium annealing temperature range, so as to provide a theoretical basis for microstructure control and processing optimisation for commercial-purity aluminium products.

Investigation of samples in the transmission electron microscope showed several phase transformations occurring during annealing in the medium temperature range. Precipitation of α_c (AlFeSi, bcc) from the matrix was observed, resulting in a fine particle dispersion. From X-ray diffraction measurements this transformation was most pronounced at an annealing temperature of 380^{o}C. Precipitation of α_c from the matrix results in a decrease in the amount of dissolved impurity elements Fe and Si, and the fine spherical particles have the least harmful effects on the plasticity. This transformation is therefore beneficial for the rolling performance of aluminium sheets.

A fine dispersion of α_c precipitates also results from the transformation of block-like or slice-like β_p (AlFeSi, monoclinic: a=8.9Å, b=4.9Å, c=41.6Å, β=92^o) precipitates (Fig. 1), beginning after a time of 4~6 hrs, and completing after about 20 hrs, for annealing at 380^{o}C. When the annealing time is prolonged to about 35 hrs at 380^{o}C, another new ternary phase, β_b (AlFeSi, monoclinic with a=b=6.12Å, c=41.5Å, β=91^o), precipitates from the matrix. The transformation of β_p to α_c leads to a decrease in the size of intermetallic particles and a reduction in the harmful effect of β_p particles on the plastic deformation of the aluminium matrix.

As the Fe/Si ratio of α_c is higher than β_p (Rivlin and Raynor 1981, Westengen 1982) transformation of β_p to α_c results in an increase in the solution of Si. On the other hand, this transformation also gives the possibility of the precipitation of β_b, decreasing the solution level of both Si and Fe. The change of the solute level of Si and Fe during annealing at 380°C was investigated using micro-hardness measurements (Fig. 2). A 'minimum solution point' was observed occurring at about 6 hrs, followed by an increase. After annealing times exceeding 20 hrs, the solution level again began to decrease, finally falling to a lower level than the 'minimum solution point'. Transformation of β_p to α_c alters the Fe/Si ratio of the aluminium solid solution, resulting in the precipitation of β_b, which in turn further decreases the solute level of Si and Fe to lower than the 'minimum solution point'.

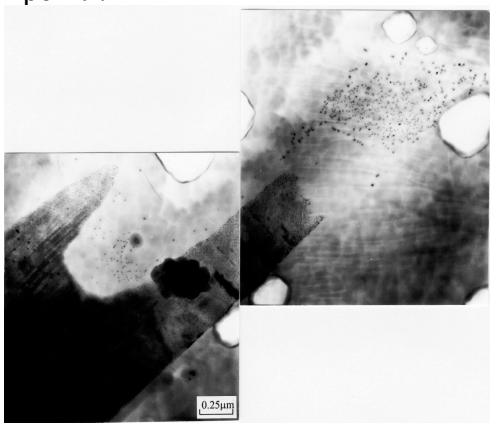

Figure 1. TEM micrograph of $\beta_p \rightarrow \alpha_c$ phase transformation.

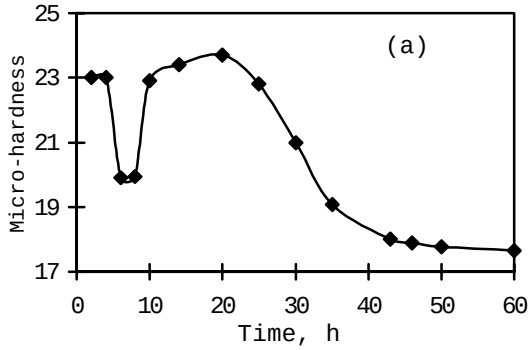

Figure 2. Hv-t curve during interstage annealing at 380°C.

References

Matsui K. (1990) Analysis of factors affecting pinhole formation in rolled aluminium foil, Kobe Steel. Kobe Res. Dev. 40(2), 89

Shoji R. and Fukijura C. (1990) Precipitation of iron and silicon in cold rolled Al-Fe-Si sheet during annealing, Key Eng. Mater. 44-45, 163

Rivlin V. G. and Raynor G. V. (1981) Critical evaluation of constitution of aluminium-iron-silicon system, International Metals Reviews 26(3), 133

Westengen H. (1982) Formation of intermetallic compounds during DC casting of a commercial purity Al-Fe-Si alloy, Z. Metallkde. 73(6), 360

In-situ TEM observation of crack propagation in 304l steel during tensile deformation

Jinwu Zhang, Puling Nie and Mei Yao

Yanshan University, Qinhuangdao, 066004 Hebei, P. R. China

The crack propagation processes under tension in foils of single phase FCC austenite stainless steel 304L(0.01C-18.5Cr-9.5Ni-1.05Mn) were studied *in-situ* in the transmission electron microscope (TEM). Slices cut with dimensions of 0.5mm(thick)×3mm×6mm were thinned to 35-50μm. Then, thin foil specimens for TEM observation were prepared using a double-jet electrolytic polishing method. In the centre of every specimen, a hole with diameter from 0.5mm to 1mm was formed. More then 100 specimens have been observed *in-situ* under continuous tension on the TEM H-800. It has been detected that after initiation at the edge of the hole, the crack propagates either by a zigzag way or by a continuous way.

As examples, the processes of crack propagation in two specimens with $(\bar{1}10)$ crystallographic plane perpendicular to electron beam are given here in detail. The relationships between the crystal orientation and the direction of tensile axis F in these two cases, as well as the crack propagation routes, are shown in Figures 1a (zigzag way) and 1b (continuous way).

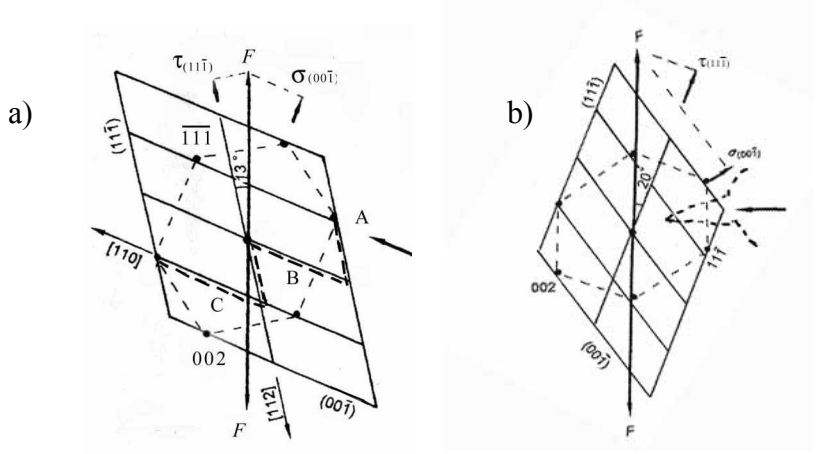

Figure 1: Crack propagation routes in (a) zigzag and (b) continuous fashion.

Typical photos showing the features of zigzag mode of crack propagation are given in Fig. 2. Figure 2a shows the dislocation free zone (DFZ) formed ahead the crack tip **O**. Micro-twins **T1**, **T2** and **T3** and contrastive lines can be seen in the DFZ. Figure 2b shows a newly formed crack

A, which appeared suddenly under tension and then arrested by twin boundaries. This crack is not connected with the original crack and is initiated at an intersecting point of the twin boundary T1 and a contrastive line.

Eventually the crack A is broadened and connects with the original crack. At the same time other cracks (B-E in Fig 2c) also begin to form in neighbouring twins that again join up with the original crack in the same manner. The repetition of such processes causes the zigzag propagation of crack (Fig. 2c).

A typical example showing the features of continuous mode of crack propagation is given in Fig 2d. The crack propagates with repetitive occurrence of blunting - developing (and re-sharpening) of the original crack. The crack keeps continuous, although its direction may be changed. It is believed that the way of crack propagation is determined mainly by the relationship between the orientation of crystal and the direction of tension axis.

From Fig. 1a, in which the crack propagation with the zigzag mode, it can be concluded that the cracks appeared suddenly under tension are developing along the crystal plane $(00\bar{1})$ and the direction of tension axis lies between the directions of $(00\bar{1})$ and $(11\bar{1})$. While for crystal in which crack propagates with the continuous mode (Fig.1b), the direction of tension axis lies outside of the angle consisting of directions $(00\bar{1})$ and $(11\bar{1})$. This conclusion is verified by other experiments carried out by us.

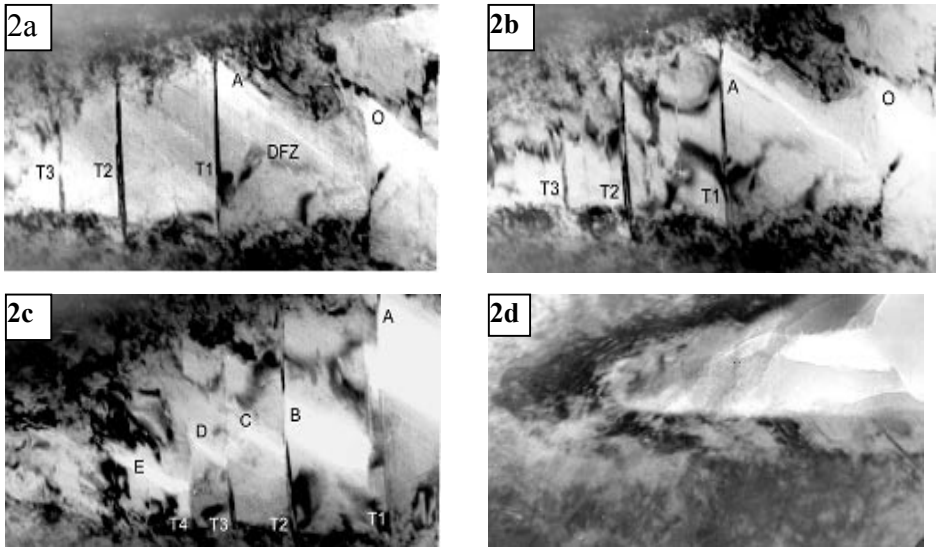

Figure 2: (a-c) crack propagation in zigzag manner by the repeated joining up to the original crack (O) by cracks (A-E) forming in neighbouring twins (T1,T2,T3) ahead of the dislocation free zone (DFZ); (d) example of crack propagation by a continuous mode.

Effects of external electric field on precipitation of AlN and recrystallization texture of deep drawing 08Al killed steel sheet

Liang Zuo, Zhuo-chao Hu and Xiang Zhao

School of Materials and Metallurgy, Northeastern University, Shenyang 110006, P.R. China

A cold rolled (73%) 08Al killed steel sheet of 1.1mm thickness was used with chemical compositions as follows: 0.009 C, 0.004 Si, 0.50 Mn, 0.04 P, 0.04 S, 0.06 Al, with Fe as the rest (wt.%). Samples were annealed at a temperature of 550°C, corresponding to the precipitation temperature AlN in this material, for 30min, 120min and 240min without or with a DC electric field of 3kV/cm. Some specimens annealed at 550^0C for 120min, were additionally annealed at 750^0C for 180min without or with electric field. The annealing treatments were done in a nitrogen atmosphere.

Selected area electron diffraction in the TEM of annealed samples confirmed the precipitation of hexagonal AlN in the samples. After 30 minutes at550deg.C the sample annealed with electric field shows more precipitation of AlN compared to the sample annealed without electric field, with the precipitates arranged along grain and subgrain boundaries. Similarly after longer annealing times at 550deg.C samples annealed with electric field again show more AlN precipitation, with also a more uniform arrangement of the AlN particles along the boundaries.

After annealing at 550°C for 120min (Figure 1), some new recrystallised grains appeared in the specimen annealed without electric field, whereas no recrystallisation was seen in samples annealed with electric field annealing. Annealed-only specimens show much more polygonized structures with flat boundaries with no or few dislocation tangles. On the contrary specimens annealed with electric field, still show cell structures with dense dislocation tangling in the boundaries and in the interior of the cells. These phenomena indicate that the AlN particles precipitated are dispersed along the boundaries during electric annealing, retard the mobility of dislocations, postpone the process of polygonization, and further restrain the subgrain formation. It is deduced therefore that the electric field annealing retards the recovery and recrystallisation processes.

Texture measurements on the two-step annealed samples (550°C+750°C) show that the gamma-fibre intensity is stronger, and the alpha-fibre texture weaker, in specimens annealed with electric field (Figure 2).

Comparing the behaviour of cold-rolled 08Al killed steel sheet samples annealed with and without electric field the following conclusions can be made;

- electric field annealing increases precipitation of the second phase-AlN and increases the uniformity of particle dispersion along grain and sub-grain boundaries
- as a result of the effect on the AlN precipitates, electric field annealing leads to an increase in the intensity of γ-fiber texture.

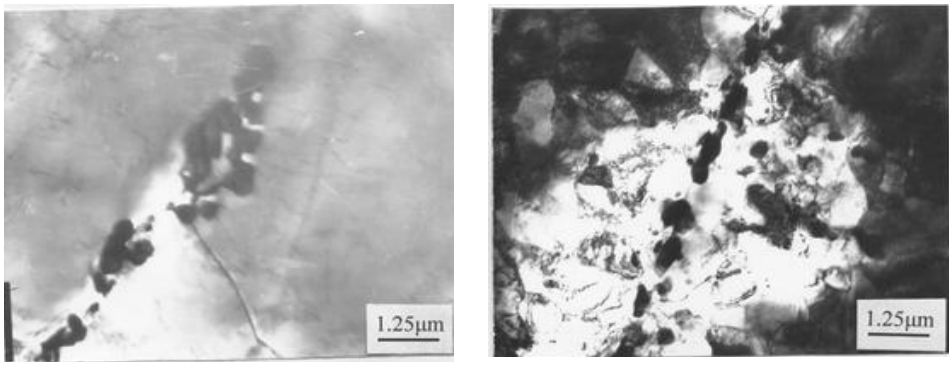

(a) (b)

Figure 1. TEM micrographs of specimens annealed at 500℃ for 120 minutes; (a) without electric field, (b) with electric field (E=3kv/cm).

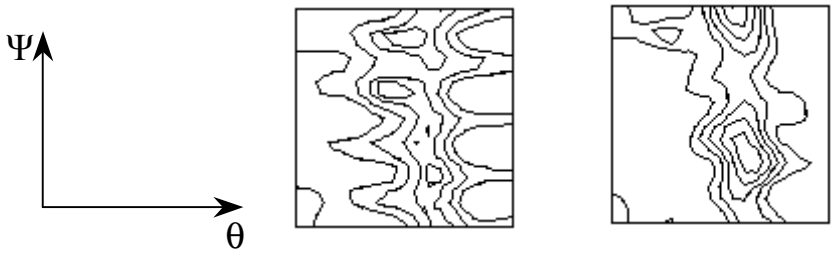

(a) (b)

Figure 2. φ=45° ODF sections of two-step annealed specimens; (a) without electric field, (b) with electric field (E=3kV/cm).

Author Index

Appendix

Summer School 'Geometry of Microstructures'

Programme

Friday, August 16	Saturday, August 17	Sunday, August 18
0830-0930 Boundaries (Ralph)	0830-0930 Boundaries (Ralph)	0830-0930 Boundaries (Ralph)
0930-1015 Stochastic Geometry (Kurzydłowski)	0930-1015 Stochastic Geometry (Kurzydłowski)	0930-1100 Microstructures in TEM (Barlow)
1015-1045 Refreshments	1015-1045 Refreshments	1100-1130 Refreshments
1045-1215 Stochastic Geometry (Kurzydłowski)	1045-1215 Stochastic Geometry (Kurzydłowski)	1130-1300 High Spatial Resolution and Analytical EM (Zhu)
1215-1530 Lunch	1215-1530 Lunch	1300 Lunch and Visit to Chi- nese Wall
1530-1630 Boundaries (Ralph)	1530-1700 Orientations (Morawiec)	
1630-1715 Orientations (Morawiec)		
1715-1745 Refreshments	1700-1730 Refreshments	
1745-1900 Orientations (Morawiec)	1730-1900 Textures (Mao)	
1900 Dinner	1900 Dinner	

Lecturers

Boundaries	Prof. Brian Ralph Brunel University Uxbridge
Stochastic Geometry / Stereology	Prof. Krysztof J. Kurzydlowski Warsaw University of Technology
Orientations	Prof. Adam Morawiec Polish Academy of Sciences Krakow
Textures	Prof. Weimin Mao University of Science and Technology Beijing
Microstructures in TEM	Dr. Claire Barlow Cambridge University
High Spatial Resolution and Analytical EM	Prof. Jing Zhu Tsinghua University Beijing

Bibliographic Data Sheet **Risø-R-1347(EN)**

Title and authors

First Joint Chinese-Danish Symposium: Characterisation of Microstructures Extended Abstracts

Jacob R. Bowen, Andy Godfrey, Wolfgang Pantleon

ISBN	ISSN
87-550-3072-6; 87-550-3073-4(Internet)	0106-2840

Department or group	Date
Center for Fundamental Research: Metal Structures in Four Dimensions	August 2002

Groups own reg. number(s) Project/contract No(s)

Sponsorship

Danmarks Grundforskningsfond and The Chinese National Science Foundation

Pages	Tables	Illustrations	References
85	1	39	87

Abstract The First Chinese-Danish Symposium on the Characterisation of Microstructures was held in Qinhuangdao, Hebei, China between 19-20 August 2002. This symposium was organised together with the closely related Summer School on the Geometry of Microstructures, which was held immediately prior to this symposium. At the symposium 29 lectures were presented and this document collects the extended abstracts from these presentations. The symposium was organised in six sessions: two on the characterisation of deformation microstructures, one on the characterisation of recrystallisation and three sessions describing the state-of-the-art of the available metallurgical techniques for the characterisation of the microstructures that occur as a result of thermomechanical processes. Under the theme of deformation, papers were presented on microstructure resulting from conventional forming processes as well as nano scale microstructures in metals such as aluminium and steel alloys produced by techniques such as surface mechanical attrition and equal channel angular extrusion. Classical aspects of recrystallisation such as stereology were presented which were then extrapolated for use in automated characterisation techniques, namely EBSP and 3DXRD, and in the same context the novel effects of magnetic and electric fields on recrystallisation phenomena were also presented. Three main techniques were intensely investigated, namely TEM, EBSD and 3DXRD and occupied half of the scope and time of the symposium. Papers ranged from cautionary notes on the use of established techniques (TEM and EBSP) to exploratory studies on the capability of the novel 3DXRD technique. This symposium provided a platform for the open discussion between Chinese and Danish scientists on various metallic microstructures and related phenomena riding on the back of a school acutely focused on the theories behind the available characterisation tools. Therefore, this report provides a snapshot of Chinese and Danish scientific efforts in the field.

Descriptors INIS/EDB